miRNA/mRNA analysis of increased TGF-β pathways drive epithelial-mesenchymal transition and regulatory T cell differentiation

Running title: miRNA/mRNA analysis links TGFβ to EMT and Tregs in Chlamydia

Authors: Toni Darville[1#], Xuejun Sun[2#], Yu Zhang[2], Catherine M. O'Connell[1], Neha Mokashi[1,2], Weiming Tang[3], Aakash Bhardwaj[1], Bryce Duncan[1], Charles W. Andrews, Jr.[4], Harold Weisenfeld[5], and Xiaojing Zheng[1,2*]

1. Department of Pediatrics, University of North Carolina at Chapel Hill, Chapel Hill, NC
2. Department of Biostatistics, University of North Carolina at Chapel Hill, Chapel Hill, NC
3. Department of Medicine, University of North Carolina at Chapel Hill, Chapel Hill, NC
4. Pathology consultant, Newburyport, MA
5. The University of Pittsburgh School of Medicine and the Magee-Womens Research Institute, Pittsburgh, PA

#: shared first authorship

*Correspondence: Xiaojing Zheng, PhD, University of North Carolina at Chapel Hill, 4018A Mary Ellen Jones Building, CB# 7509, 110 Manning Drive, Chapel Hill, NC 27599-7509, USA

This revision updates the preprint to a non-reusable license that restricts redistribution and reuse; no changes were made to the scientific content

Abstract – 249 words (limit 250 words)

Chlamydia trachomatis genital tract infection is linked to severe reproductive complications in women, including ectopic pregnancy, infertility, and adverse pregnancy outcomes. Mouse models of infection suggest that chlamydia-induced dysregulation of microRNAs (miRNAs) can drive harmful cytokine responses, pathogenic epithelial-mesenchymal transition (EMT), and fibrosis. To investigate these mechanisms in humans, we profiled miRNA and mRNA expression in endometrial biopsies from women with endometrial infection (Endo+) and compared them to profiles from women with cervix-only infection (Endo-) or no infection. Ingenuity Pathway Analysis (IPA) revealed that Endo+ tissues had upregulated genes associated with innate and adaptive immune response pathways, as well as EMT regulation, while downregulated genes were linked to cell cycle control. An integrative miRNA-mRNA analysis, which combined a review of published miRNA regulation in human infections and immune responses with IPA's miRNA target filter, identified differentially expressed miRNAs that modulate these pathways in the endometrium of Endo+ women. Functional annotation of these miRNAs showed a predominance of downregulated miRNAs that typically suppress EMT and regulatory T cell (Treg) differentiation, along with miRNAs that usually enhance Th17 responses. Comparisons with previously identified mRNA pathways in blood samples from women with endometrial *Chlamydia* infection indicated that alterations in TGF-β signaling and EMT were specific to the endometrium. Overall, the miRNA-mRNA interactions inferred from Endo+ tissue suggest increased activity in TGF-β pathways that promote enhanced EMT and Treg differentiation, while reducing Th17 activation. These changes highlight a dual potential for promoting tissue scarring while dampening inflammatory responses that could otherwise limit infection.

50 **Introduction**

51 Sexually transmitted *Chlamydia trachomatis* (Ct) genital infections represent a global public
52 health challenge due to their high prevalence and severe reproductive health consequences. These
53 include pelvic inflammatory disease (PID), chronic pelvic pain, infertility, and ectopic pregnancy
54 (1, 2). Infertility and ectopic pregnancy after Ct infection is primarily caused by fibrotic scarring
55 of the oviducts. Additionally, studies have linked Ct with adverse pregnancy outcomes such as
56 stillbirth, infant death, spontaneous abortion, preterm labor, small-for-gestational-age infants, and
57 postpartum endometritis (3). This suggests that Ct may cause lasting endometrial damage.

58 In the female reproductive tract, immune cells in the vagina and cervix provide the first line of
59 defense against infection, whereas immune cells in the endometrium play a dual role: eliminating
60 pathogens that breach the cervical barrier and maintaining immune tolerance of the embryo during
61 pregnancy. Regulatory T (Treg) cells in the uterus are critical for immune tolerance to foreign fetal
62 antigens(4, 5). Their secretion of anti-inflammatory cytokines such as IL-10 and TGF-β, and
63 expression of inhibitory molecules like CTLA-4 and PD-1, suppress maternal immune responses
64 that could otherwise target the fetus. In contrast, Th17 cells drive proinflammatory responses that
65 can be harmful. The balance between these cell types is crucial for a healthy pregnancy. During
66 Ct infection, the induction of Tregs may hinder the development of effective T cell immunity (6),
67 whereas the activation of chlamydial-specific Th17 cells appears to enhance resistance to
68 reinfection (7). Therefore, while a higher Treg/Th17 ratio supports reproductive health, it may
69 compromise host defense against Ct.

70 Animal models have also shown that pro-inflammatory signaling and immune cell recruitment are
71 initiated upon Ct infection of host epithelial cells (8, 9). Engagement of pathogen recognition
72 receptors (PRRs) elicits a rapid influx of neutrophils that fail to kill the bacteria while releasing

73 tissue-damaging molecules such as reactive oxygen species and matrix metalloproteases (10-15).
74 Eventually, chlamydia-specific IFN-γ-producing CD4 T cells, activated by dendritic cells, resolve
75 infection. However, danger-associated molecular patterns (DAMPs) released by chlamydiae or
76 dying epithelial cells can perpetuate inflammation through induction of production of TNFα and
77 IL-1α by adjacent epithelium or influxing innate cells, creating a feed-forward loop of tissue
78 damage (11, 16, 17). Furthermore, epithelial-mesenchymal transition (EMT)—a dysregulated
79 tissue repair process controlled by microRNAs (miRNAs)—has been implicated in oviduct fibrosis
80 in chlamydia-infected mice (18). During EMT, epithelial cells lose cell-cell contacts and acquire
81 mesenchymal characteristics, including elevated production of extracellular matrix proteins,
82 before transitioning into myofibroblasts.

83 Mouse models of chlamydial infection demonstrated that the induction of EMT involves TNFα
84 signaling, caspase activation, and cleavage inactivation of Dicer (18, 19) an RNase III enzyme that
85 processes RNA into microRNAs. MicroRNAs (miRNAs) are small non-coding RNAs that play a
86 crucial role in post-transcriptional gene regulation, primarily through translational repression and
87 mRNA degradation. However, miRNAs can also enhance gene expression and translation under
88 certain conditions (20, 21). miRNAs are predicted to control the activity of approximately 30% to
89 50% of all protein-coding genes. A single miRNA can target multiple mRNAs, while multiple
90 miRNAs can collaborate to finely tune the expression of a single mRNA target (22). Chlamydia
91 infection in mice was associated with reduced expression of miRNAs that normally suppress EMT,
92 fibrosis and tumorigenesis, alongside increased expression of proteins associated with EMT and
93 fibrosis (18, 19)

94 Human salpingeal tissues are challenging to obtain but minimally invasive endometrial suction
95 catheter biopsies can be collected in an office setting (23). Histological evidence of endometritis

correlates with salpingitis observed via laparoscopy (24) and is associated with an increased risk of infertility in women with symptomatic or asymptomatic Ct infection (25). Histologic features resembling endometritis have also been described in surgically removed Fallopian tubes (26), supporting the use of endometrial biopsies for investigating pathogenic mechanisms underlying Ct-induced disease.

In this study, we conducted an integrated analysis of endometrial mRNA and miRNA profiles in cisgender women with high exposure to Ct. Our findings identified an infection-driven mRNA signature that highlights active innate and adaptive immune signaling pathways, along with epithelial-mesenchymal transition (EMT), in women with endometrial Ct infection compared to those with cervical Ct infection only and uninfected women. A parallel miRNA analysis revealed significant downregulation of several miRNAs that typically suppress mRNAs involved in activating TGF-β-related pathways, which drive EMT and regulatory T cell (Treg) differentiation. Additionally, a partially overlapping subset of miRNAs that typically enhance proinflammatory Th17 differentiation was also downregulated. The suppression of these miRNAs during endometrial Ct infection appears to release their regulatory effects, facilitating EMT and increasing the potential for tissue scarring. However, the miRNA-mediated shift in the Treg/Th17 balance, favoring Tregs, may simultaneously act to dampen inflammation.

118 **Materials and Methods**

119 ***Ethics statement.*** This study adhered to the Declaration of Helsinki guidelines, and all participants
120 provided written informed consent prior to participation. The study protocols were approved by
121 the Institutional Review Boards for Human Subjects Research at the University of North Carolina
122 and the University of Pittsburgh.

123 ***Study population***. Endometrial biopsy samples were obtained from cisgender female participants
124 enrolled in two independent cohorts with high exposure to Ct infection. Anaerobes and Clearance
125 of Endometritis (ACE) Cohort: Participants were women clinically diagnosed with pelvic
126 inflammatory disease (PID) (27, 28). Diagnostic criteria for enrollment included cervical motion
127 tenderness, uterine tenderness, or adnexal tenderness observed during pelvic examination in
128 sexually active young women experiencing pelvic or lower abdominal pain. T Cell Response
129 Against Chlamydia (TRAC) Cohort: Participants were asymptomatic women identified as being
130 at high risk for Ct infection (29). At enrollment, demographic, behavioral, and medical history data
131 were collected. General physical and pelvic exams were conducted, and blood samples were
132 obtained for immune studies. Participants underwent endometrial biopsy sampling using suction
133 catheters. Additional assessments included Gram-stained vaginal smears for bacterial vaginosis
134 using Nugent scores (30), as well as testing for Ct, *Neisseria gonorrhoeae* (Ng), and *Mycoplasma*
135 *genitalium* (Mg) in cervical swabs and endometrial biopsies using nucleic acid amplification tests.
136 Histopathological analyses of biopsies were performed (25, 31).

137 Participants were categorized into three primary groups based on infection status: (1) Endo+: Ct
138 detected in both the endometrium and cervix. Endo+ women were further categorized into
139 subgroups of women with clinical PID (Endo+, PID+), and asymptomatic women (Endo+, PID-).
140 (2) Endo-: Ct detected in the cervix only, without endometrial infection. (3) Uninfected: No Ct

141 infection. For miRNA analyses, women with PID-like symptoms with negative tests for Ct, Ng,
142 and Mg were included as an additional comparison group.

143 ***Study design and workflow.*** The study workflow is depicted in **Figure 1**. Endometrial biopsy
144 samples were analyzed for mRNA and miRNA expression. Principal Component Analysis (PCA)
145 was used to explore transcriptomic relationships among cohort participants. Differentially
146 expressed (DE) mRNAs and miRNAs were identified between Endo+ and Endo-/Uninfected
147 groups. Functional annotations of DE mRNAs and miRNA-mRNA pairs were conducted using
148 Ingenuity Pathway Analysis (IPA). Endometrial mRNA data were also compared with previously
149 published blood mRNA data from the same cohorts (32).

150 ***mRNA and miRNA data collection and processing***. mRNA Extraction and Profiling: Total RNA
151 was extracted from endometrial biopsies stored at -80°C in tubes containing RNA/DNA Shield
152 (Zymo Research, Irvine, CA). After thawing, samples were weighed, minced, and processed for
153 simultaneous DNA and RNA extraction using the Quick DNA/RNA™ isolation kit according to
154 the manufacturers protocol (Zymo) with on column DNAse I treatment prior to total RNA elution.
155 Libraries were prepared using the Ovation SoLo RNA-Seq kit (NuGen Technologies) and
156 sequenced on an Illumina HiSeq2500 platform in the High Throughput Sequencing Facility (HTSF)
157 at the University of North Carolina. Gene expression quantification used BBMap (v37.25) and
158 samtools (v1.4.1). Blood mRNA pathway data had been previously generated by microarray
159 hybridization analysis using samples obtained from ACE and TRAC participants (31, 32). miRNA
160 Extraction and Profiling: miRNAs were isolated using HTG EdgeSeq reagents according to the
161 user manuscript, and libraries were synthesized at the HTSF at the University of North Carolina.
162 Barcoded samples were pooled, and sequencing was performed on an Illumina NextSeq 500

163 platform using a 75-cycle High Output v2 kit. Count data were generated by the EdgeSeq parser
164 software (HTG Molecular Diagnostics, Inc.).

165 ***Data accession***. All endometrial mRNA and miRNA profiles have been deposited in the Gene
166 Expression Omnibus database (https://www.ncbi.nlm.nih.gov/geo/) GEO accession number:
167 GSE290615 for endometrial mRNA, and GSE289941 for endometrial miRNAs. The blood mRNA
168 profiles were retrieved from the previous study (32) with GEO accession number GSE110106.

169 ***Statistical analysis***. Demographic Data: One-way ANOVA was used for numerical variables,
170 while Fisher's exact test or Chi-square test was applied for categorical variables. RNA-Seq Data:
171 PCA with ComBat-seq (33) correction was applied to address batch effects. mRNAs with
172 expression levels <20 in >50% of samples were excluded, leaving 16,183 mRNAs for analysis.
173 miRNAs with expression levels below mean +3 standard deviations of negative controls were
174 filtered, retaining 253 miRNAs. Normalization was performed using DESeq2 (v1.36.0) (34). PCA
175 of variance by R was used to identify the inherent pattern of samples. Differential Expression
176 Analysis: DE mRNAs and miRNAs were identified using DESeq2 with false discovery rate (FDR)
177 <0.05. All analyses, unless specified, were completed in R (version 4.1.0). Within-sample group
178 clustering heatmaps were generated to visualize DE miRNA expression across groups.

179 ***Functional annotation and pathway enrichment analysis of mRNAs.*** Ingenuity Pathway
180 Analysis (IPA) (QIAGEN Inc., https://digitalinsights.qiagen.com/IPA) identified enriched
181 pathways for DE mRNAs, using Fisher's exact test. Regulatory T cell-related mRNAs not included
182 in IPA were sourced from Gene Ontology (GO) (35) and manually curated from literature.

183 ***Integrated miRNA-mRNA analysis***. Putative target mRNAs of DE miRNAs were identified
184 through IPA's "miRNA target filter" which incorporates both published experimental and high-

185 confidence computational data. mRNA targets were further filtered to include only those that were
186 also identified as DE mRNAs (FDR<0.05) in this study. We performed a functional annotation of
187 the negatively correlated miRNA-mRNA pairs to identify significantly enriched pathways.

188 ***Systematic review of miRNA functions***. A systematic review identified studies examining DE
189 miRNA functions in human immune-related processes. PubMed searches from 1990 to 2024 used
190 the following search query: all miRNAs AND (infect OR immune OR autoimmune) AND (human
191 OR patient OR healthy donor) AND ("T cell" OR "B cell" OR lymphocyte OR CD4 OR CD8 OR
192 Treg OR Th1 OR Th2 OR Th17 OR Tfh OR neutrophil OR monocyte OR macrophage OR "NK
193 cell" OR "epithelial cell" OR "dendritic cell") AND (expression OR function OR Differentiation
194 OR activated OR activation OR inhibit OR suppress OR stimulation) NOT ("beta-cell" OR
195 methylation OR stem OR endothelial OR pregnancy). Tumor-related and non-immune studies
196 were excluded, leaving 361 full-text studies curated for miRNA effects on immune and epithelial
197 cell responses including directionality of their effects.

198 ***Comparison of DE mRNA enriched pathways detected in the endometrium versus blood.*** We
199 previously identified blood DE mRNAs from women with Ct-induced pelvic inflammatory disease
200 (PID) (Endo+) to those from asymptomatic women with cervical infection only and uninfected
201 women (Endo-/Uninfected) (32). Using Bonferroni-adjusted P values <0.05 as the significance
202 threshold, we compared the significantly enriched pathways for DE mRNAs from this endometrial
203 study and the aforementioned blood study.

204

205

206

207 **Results**

208 ***Characteristics of study participants.*** The characteristics of study participants included in the
209 mRNA (N = 15) and miRNA (N = 23) analyses are summarized in **Supplementary Tables 1 and**
210 **2**. Participant group sizes were determined by the quality of mRNA and miRNA isolated from
211 tissue specimens. Most participants were young, African American, unmarried, had some college
212 education, and were insured by Medicaid. A majority reported previous Ct infection, had anti-Ct
213 antibodies, and did not have bacterial vaginosis (BV) by Nugent's criteria (30) or coinfection with
214 Ng and/or Mg. Demographic variables such as age, race, education, insurance status, and
215 contraceptive use did not differ significantly among groups.

216 ***Distinct gene expression profiles in Endo+ women contrast with minimal impact of cervical Ct***
217 ***infection***. Unsupervised principal component analysis (PCA) was performed to assess whether
218 global gene expression profiles were associated with infection status or disease extent. PCA of
219 mRNA data (**Figure 2A**) showed that most Endo+ women formed a distinct cluster, separate from
220 the Endo- and Uninfected groups, with one outlier in the Endo+ group. Similarly, PCA of miRNA
221 data (**Figure 2B**) indicated that Endo+ women clustered apart from the Endo- and Uninfected
222 groups. However, PCA did not detect differences between endometrial mRNA or miRNA
223 expression profiles of women with cervical Ct infection or those who were uninfected. The lack
224 of separation between Endo- and Uninfected groups suggests that cervical Ct infection does not
225 significantly impact endometrial gene expression.

226 ***Endometrial inflammation was detected in Endo+ and non-STI PID cases.*** Biopsied tissues from
227 Endo+ women, both symptomatic and asymptomatic, and from women with non-STI-induced PID
228 showed plasma cell and lymphocyte infiltrates in the endometrial stroma. Neutrophils were also
229 observed within the basal lamina of the epithelium and in gland lumens in some Endo+ biopsies.

230 In contrast, 6 evaluable biopsis from women with cervical Ct infection only and 9 evaulable
231 biopsies from uninfected women either lacked inflammatory cells or contained rare mononuclear
232 cells. The remaining biopsies had insufficient tissue for histological evaluation (**Figure 3A-D**).
233 These pathological data align with the data from PCA analysis indicating clear separation of
234 endometrial transcriptional profiles of Endo+ women from those with Ct infection limited to the
235 cervix.

236 ***Key transcriptional differences in Ct endometritis highlight induction of innate and adaptive***
237 ***immune responses, EMT, and cell cycle dysregulation that is confirmed by functional analysis***
238 ***of miRNA-mRNA interactions***. Since PCA showed minimal variance between the Endo- and
239 Uninfected groups, their transcriptional data were combined and compared to the Endo+ group. A
240 total of 2,000 mRNAs were significantly DE between Endo+ and Endo-/Uninfected groups (FDR
241 < 0.05), with 1046 upregulated, and 954 downregulated genes in the Endo+ group. The top 100
242 upregulated and downregulated genes with FDR <0.05 are listed in **Supplementary Tables 3 and**
243 **4**, respectively and displayed in a volcano plot (**Figure 4**).

244 Several of the most strongly upregulated genes play crucial roles in local antibody production and
245 germinal center formation. These include transcription factors and coactivators such
246 as *BCL6* and *POU2AF1*, *CXCL13*, a key germinal center chemokine, and antibody Fc receptors
247 including *FCAR*, the IgA receptor, and *FCRL2*, which supports B cell antibody production
248 (**Supplementary Table 3**). This gene expression pattern was consistent with the marked plasma
249 cell infiltrates observed in women with PID, underscoring the hallmark histology of chronic
250 endometritis (**Figure 3A-B**) (36-40). Other highly upregulated genes are involved in the acute
251 phase response and cytokine cascade along with secondary mediators, including chemokines,

252 colony-stimulating factors, and prostaglandins, which amplify leukocyte recruitment and local
253 innate immunity (*IL1B*, *IL1RN*, *IRAK3*, *GSDMC*, *C2CD4A*, *CSF3R*, *CXCL1*, *SOD2*, *PTGS2*)
254 (**Supplementary Table 3**). *PTGS2* which encodes a cyclooxygenase enzyme that catalyzes
255 prostaglandin synthesis and is linked to pain, was up-regulated in Endo+ women, some of whom
256 exhibited PID symptoms.

257 Upregulated pathways identified by IPA included non-specific inflammatory responses (acute
258 phase response, PPARa/RXRa activation, *IL-6*, *PI3K/AKT*, *JAK/STAT*), innate (*TREM1*, NK cell,
259 nitrous oxide, phagosome formation, Toll-like receptor (TLR) and pattern recognition receptor
260 (PRR) signaling, granulocyte adhesion, and HMGB-1 signaling), and adaptive immune response
261 pathways (*IL-10*, Th1/Th2, CD40 signaling, IL-9 signaling) (**Figure 5A, Supplementary Table**
262 **5**).

263 IPA also identified EMT pathway enrichment, driven by upregulation of *TGFB2*, *TGFBR2*,
264 *SMAD3*, and *ZEB2* (**Figure 5A, Supplementary Table 5)**. *TGFB2* interacts with its receptor to
265 activate SMAD proteins, including SMAD3. This activation promotes the expression of EMT-
266 related genes such as *ZEB2*, a transcription factor which represses epithelial markers like E-
267 cadherin and enhances mesenchymal markers, playing a pivotal role in EMT progression.

268 Downregulated genes included membrane adhesion components (*GJB6*, *CDH10*, *PCDH10*) and
269 tissue remodeling enzymes (*MMP26*, *FBN3*, *PLOD1*), as well as genes involved in transcription
270 regulation (*RXRG* and *SPDEF*), protein synthesis (*DHFR*, *GSTZ1*) and modification (*APRT*,
271 *RYCR1*), and cellular metabolism (*KMO*, *NDUFB7*, *UQCRC1*) (Supplementary Table 4). Multiple
272 genes related to histone metabolism were also decreased, potentially altering chromatin structure
273 and impacting gene expression regulation (**Figure 4 and Supplementary Tables 4 and 6**).

274 Downregulated pathways were enriched in genes involved with cell cycle regulation,
275 mitochondrial dysfunction, and nucleotide biosynthesis (**Figure 5B, Supplementary Table 6**).

276 Consistent with the DE mRNA results (**Figure 5A**), functional enrichment analysis using IPA
277 revealed that downregulated miRNA-mRNA interactions in Endo+ women enriched pathways
278 such as "Regulation of EMT by Growth Factors" (**Figure 5C**, **Supplementary Table 7**),
279 highlighting EMT promotion. Additionally, these interactions enriched pathways containing
280 upregulated innate and adaptive immune signaling genes (**Figure 5C**). In contrast, upregulated
281 miRNAs associated with downregulated mRNAs were enriched in pathways involving cell cycle
282 regulation and DNA damage signaling (**Figure 5D**), aligning with mRNA findings (**Figure 5B**
283 **and Supplementary Table 8**). These results suggest that Ct infection decreases the transcription
284 of miRNAs that normally suppress EMT and immune signaling genes, potentially accelerating
285 scarring and inflammation. Simultaneously, the infection increases the transcription of miRNAs
286 that downregulate mRNAs involved in mucosal epithelial homeostasis, possibly further impairing
287 uterine healing processes.

288 ***Differential expression of miRNAs highlights EMT promotion and Treg/Th17 modulation in***
289 ***endometrial Ct infection.*** A total of 89 miRNAs were significantly DE (FDR<0.05) between
290 Endo+ and Endo- women. Among these, 47 miRNAs were upregulated, and 42 were
291 downregulated (**Supplementary Tables 9 and 10).** miRNAs with fold changes >2 and <1/2 are
292 depicted in **Figure 6A**. The majority of (53 of 89) DE miRNAs were associated with EMT with
293 32 miRNAs that normally dampen EMT being downregulated and 4 that increase EMT being
294 upregulated (**Figure 6B**), leading to an overall effect of enhancing EMT (**Table 1**).

295 IPA's target filter and literature review identified target mRNAs linked to TGF-β signaling, crucial
296 for EMT induction. These included *JAK1/STAT3* (103), Smad-dependent and (104) independent

297 *TGF-β* pathways, and the autocrine signaling network for EMT involving *TGF-β* and *ZEB2* (104).
298 Transcription factors (e.g., *ZEB2*, *FOXO1*) and pathways like PI3K-AKT were upregulated,
299 emphasizing EMT promotion. Among the 25 most significantly downregulated miRNAs in Endo+
300 samples, seven (miR-141-3p, miR-200a-3p, miR-106b-5p, miR-224-5p, miR-20a-5p, miR-21-5p,
301 and miR-223-3p) were identified through literature review as directly suppressing *TGF-β*
302 production. Consequently, their downregulation in Endo+ women likely enhances *TGF-β* activity,
303 which may suppress chronic inflammation but also promote EMT, potentially contributing to
304 adverse pathological outcomes.

305 Among the 89 differentially expressed (DE) miRNAs, 32 were associated with T cell regulation,
306 including subclasses such as Tregs, Th17, and Th1. *TGF-β* plays a key role in the differentiation
307 of both Tregs and Th17 cells. However, the presence of additional cytokines, particularly
308 interleukin-6 (*IL-6*), shifts differentiation toward Th17 cells. Specifically, low *TGF-β*
309 concentrations combined with *IL-6* promote Th17 differentiation, whereas high *TGF-β* levels
310 suppress *IL-6* signaling and favor Treg differentiation (105).

311 Twenty miRNAs were linked to Treg differentiation, with 12 downregulated miRNAs typically
312 functioning to suppress Tregs (**Figure 6C, Table 2**). Notably, miR-146a-5p, which promotes
313 Tregs, was upregulated, while miR-148a-3p, another Treg-enhancing miRNA, was reduced. These
314 expression patterns suggest an overall increase in Treg differentiation in Endo+ women.

315 For Th17 differentiation, 25 miRNAs were identified (**Figure 6D, Table 3**). Of these, 14 miRNAs
316 that typically enhance Th17 cells were significantly reduced, 10 of which also function to suppress
317 Tregs. Additionally, two miRNAs that normally inhibit Th17 differentiation were upregulated.
318 Conversely, six miRNAs that suppress Th17 differentiation were downregulated, and miR-149-

319 3p, which promotes Th17 cells, was increased. Overall, 16 of the 25 DE miRNAs are predicted to
320 reduce Th17 differentiation, while 7 are associated with increased Th17 differentiation.

321 Several target mRNAs were linked to promoting Treg differentiation over Th17 cells. These
322 include transcription factors such as *FOXO1*, *RUNX1*, *IRF1*, and *BATF*, as well as key *TGF-β*
323 pathway genes (*TGFBR2*, *SMAD3*, *STAT5*, *STAT3*, and *IL-10R*). Collectively, these findings
324 indicate a shift toward increased Treg activity and reduced Th17 differentiation. This shift may
325 help limit tissue-damaging neutrophil responses but could come at the cost of impaired Th17/Th1-
326 mediated protection against reinfection (7).

327 A within-sample group clustering heatmap of DE miRNAs (**Figure 7**) revealed distinct expression
328 patterns across groups: Endo+ women with and without symptoms, Endo-, Uninfected, and women
329 with non-STI-induced pelvic pain. One cluster of miRNAs was downregulated in Endo+ women
330 (symptomatic and asymptomatic) compared to Endo-, Uninfected, and women with non-STI-
331 induced pelvic pain. Literature review suggests these miRNAs typically suppress EMT (**Table 1**),
332 implying their downregulation in Endo+ women may promote EMT, regardless of symptom
333 presence. Notably, this downregulation was not observed in non-STI pelvic pain cases, suggesting
334 a link to active Ct infection (**Figure 7**).

335 However, a minor cluster of miRNAs (mir-1273, mir-1285-5p, mir-1254, mir-4734, and mir-566)
336 that normally dampen mRNAs promoting EMT (**Table 1, Figure 7**), was downregulated in Endo+,
337 4 of 5 Endo-, and 5 of 7 non-STI pelvic pain cases with recent prior Ct infection, indicating
338 potential enhancement of EMT processes irrespective of current Ct ascension or symptom status.
339 Each of these miRNAs have been studied in various cancer types, and reportedly have both positive
340 (miR-1273 (137), miR-4734) and negative roles (miR-1285-5p (138), miR-1254 (139), miR-566
341 (140)) in promoting cell proliferation, invasion, and metastasis. Furthermore, four miRNAs (miR-

342 320b (102, 141), let-7c-5p and let-7b-5p (79)) reported to induce EMT and promote oncogenesis
343 were upregulated in Endo+ women and those with non-STI-induced pelvic pain (**Table 1, Figure**
344 **7**).

345 ***Distinct immune and fibrosis-related pathways were detected in endometrial vs. blood mRNA***
346 ***profiles in women with chlamydial endometritis***. In a previous study (32), we compared blood-
347 derived mRNA profiles from women with Ct-induced pelvic inflammatory disease (PID) (Endo+)
348 to those from asymptomatic women with cervical infection only and uninfected women (Endo-
349 /Uninfected). A comparison of the top enriched pathways identified in blood with those found in
350 the endometrium of Endo+ women revealed notable differences (**Table 4**). Shared pathways
351 related to innate immune responses, including granulocyte adhesion, *TREM1* signaling, Toll-like
352 receptor (TLR) signaling, integrin signaling, *IL-1*, *IL-10*, and *IL-6* response pathways, as well as
353 *JAK/STAT* signaling. Endometrium--specific responses included natural killer (NK) cell signaling
354 pathways, *IL-23*, *STAT3*, and Th17 activation pathways which can lead to chronic inflammation if
355 excessively activated (142), multiple adaptive T cell response pathways (Th1/Th17, Th2, and *IL-*
356 *7*), and fibrosis-related pathways, *TGF-β* signaling and EMT. These sharply contrasted with the
357 blood profiles of Endo+ women, where TCR signaling pathways—including mTOR, which
358 integrates immune signals and metabolic cues for T cell maintenance and activation, and *ICOS-*
359 *ICOSL* signaling which delivers the co-stimulatory signals that promote T cell activation and
360 differentiation—were significantly downregulated, and activation of EMT pathways was
361 undetected. Conversely, type I interferon signaling pathways were prominent in blood-borne
362 profiles, but displayed minimal enrichment in the endometrium.

363

364

365 **Discussion**

366 The findings from this study improve understanding of how Ct infection modulates the molecular
367 landscape of the human endometrium, emphasizing the interplay between immune responses,
368 EMT, and regulatory miRNA activity. These results provide insight into how Ct infection may
369 contribute to adverse pregnancy outcomes, including stillbirth and preterm labor, as well as the
370 Ct-induced complication of chronic pelvic pain.

371 The integrated transcriptomic and miRNA analyses revealed distinct molecular signatures in the
372 endometrial tissues of women with endometrial Ct infection (Endo+), highlighting active innate
373 and adaptive immune signaling pathways alongside EMT promotion. The transcriptional patterns
374 of upregulated genes associated with the acute phase response as well as genes that promote
375 antibody-producing cells and cell-mediated immunity correlate with histological findings of
376 endometritis, marked by a predominance of plasma cell infiltrates mixed with subepithelial
377 neutrophils and lymphocytes. Other upregulated genes in Endo+ women, such
378 as *TGFB2*, *TGFBR2*, and *SMAD3*, collectively drive EMT through Smad-dependent and
379 independent mechanisms, while transcription factors like *ZEB2* suppress epithelial markers to
380 facilitate mesenchymal transitions. The significant downregulation of EMT-suppressing miRNAs,
381 including miR-141-3p and miR-200a-3p, further supports this shift toward EMT, aligning with
382 prior observations in murine models (18, 19, 143). These molecular alterations are consistent with
383 enhanced tissue remodeling, fibrosis, and scarring—hallmarks of the Ct-induced complications of
384 tubal factor infertility and ectopic pregnancy. The additional detection of upregulated miRNAs
385 that depress gene pathways engaged in nucleotide synthesis and cell cycle control indicate a further
386 mechanism whereby miRNA dysregulation could inhibit healing of infected endometrial tissue.
387 While this study focused on endometrial biopsy tissues, it is highly likely that similar mechanisms

388 are at work in the delicate oviduct. EMT and fibrosis in the oviduct could impair critical
389 reproductive processes, including gamete transport, fertilization, early embryo development,
390 immune defense, and structural integrity—all of which are essential for successful reproduction.

391 The enrichment of *TGF-β* signaling and its downstream transcription factors, such as *ZEB2*, in
392 Endo+ samples underscores the role of this pathway in driving EMT. Downregulated miRNAs that
393 typically suppress *TGF-β* signaling, including miR-141-3p and miR-200a-3p, likely amplify this
394 effect. These molecular changes are consistent with previous studies in mouse models, which
395 demonstrated that dysregulated EMT contributes to fibrosis and oviductal scarring. Igietseme et
396 al. (18) showed that *Chlamydia muridarum*-induced TNFα signaling and caspase activation were
397 linked to the downregulation of miRNAs that typically inhibit EMT and fibrosis. Similarly,
398 alterations in *TGF-β*, *TNF*, *ZEB*, and the miR-200 family observed in Endo+ women were also
399 identified in infertile mice, with multiple differentially expressed miRNAs involved in EMT
400 overlapping between the two studies (143, 144) demonstrated significant downregulation of
401 miRNAs that suppress fibrosis, including members of the miR-200 family in mice with oviduct
402 pathology following *C. muridarum* infection. This overlap in miRNA dysregulation between
403 human and mouse studies suggests a conserved *Chlamydia*-induced EMT mechanism across
404 species. The downregulation of these miRNAs, combined with the activation of *TGF-β* signaling,
405 likely creates a microenvironment conducive to tissue remodeling and scarring. This process may
406 represent a critical step in the progression from infection to tubal factor infertility.

407 A notable finding was the miRNA-driven shift in the Treg/Th17 balance. Among the 89 DE
408 miRNAs, many were linked to immune cell regulation, particularly promoting Treg differentiation
409 and function. The downregulation of miRNAs that typically suppress Tregs (e.g., miR-200a-
410 3p, miR-374b-5p) suggests an enhanced Treg response, potentially favoring immune tolerance at

411 the expense of effective Th1/Th17-mediated immunity. This interpretation is bolstered by the
412 upregulation of miR-146a-5p, known to support Treg function, and the increased expression of
413 Treg-associated mRNAs, such as TGFBR2 and Smad3.

414 Conversely, the downregulation of Th17-promoting miRNAs, such as miR-21-5p, miR-19b-
415 3p, and miR-223-3p, indicates a reduction in Th17 activity. Since Th17 cells enhance neutrophil
416 recruitment, decreased Th17 activity could mitigate tissue-damaging neutrophil responses, key
417 drivers of chlamydial disease pathogenesis (15). However, given Ct's intracellular developmental
418 cycle, and its production of Chlamydial Protease Activation Factor (CPAF), which impairs
419 neutrophil function (145), neutrophils have limited efficacy in eliminating Ct, and reduced
420 neutrophil activation may have little impact on infection resolution. However, Th17 cells exhibit
421 plasticity, transitioning between Th17 and Th1 phenotypes, and have been strongly associated with
422 resistance to chlamydial reinfection (7). Thus, the observed shift in the Treg/Th17 balance has
423 contrasting implications. Enhanced Treg/Th17 activity may reduce chronic inflammation and
424 preserve endometrial function; while simultaenously, impeding development of protective
425 immunity, potentially contributing to the high rates of reinfection observed in some cohort
426 participants (7). This delicate trade-off underscores the challenges of therapeutically targeting
427 these pathways, as interventions could disrupt the balance between immune suppression and
428 effective defense.

429 Comparative analyses between endometrial and previously published blood mRNA profiles
430 highlight tissue-specific responses to Ct infection. While blood profiles revealed activation of
431 interferon-mediated signaling and downregulation of adaptive T cell pathwys, endometrial
432 responses were dominated by activation of T cells (e.g., Treg, Th1, Th17), EMT, and *TGF-β*-
433 driven immune regulation. These differences underscore the localized nature of Ct-induced

434 endometrial inflammation and fibrosis, which may not be readily detectable through systemic
435 biomarkers. This localized EMT induction aligns with the histological evidence of fibrosis
436 observed in Ct-affected Fallopian tubes, suggesting a direct link between Ct gene regulation in the
437 upper genital tract and long-term reproductive sequelae. These findings underscore the importance
438 of localized studies for understanding the distinct molecular landscape of Ct-infected reproductive
439 tissues.

440 We acknowledge several limitations of this study. The sample size for the endometrial
441 transcriptome was constrained by the difficulty of obtaining sufficient high-quality endometrial
442 tissue for mRNA and miRNA profiling. Additionally, the cross-sectional design of the study limits
443 our ability to assess the temporal progression of infection and associated pathology. Future studies
444 with larger sample sizes and longitudinal designs are needed to validate these findings and provide
445 a more comprehensive understanding into the progression of Ct-induced pathology and the
446 persistence of molecular changes post-infection. Extending these analyses to other sexually
447 transmitted infections could determine whether similar miRNA-mediated mechanisms drive
448 reproductive tract inflammation and scarring across different pathogens.

449 Despite these limitations, our study provides a new and comprehensive view of molecular changes
450 in the endometrium during Ct infection, highlighting critical pathways that drive tissue remodeling,
451 fibrosis, and immune dysregulation. The findings also raise concerns about asymptomatic Endo+
452 women, who exhibited similar molecular profiles to symptomatic individuals, suggesting that
453 subclinical endometrial inflammation may contribute to reproductive morbidity, which supports
454 prior studies indicating that asymptomatic women with Ct-induced endometritis have an increased
455 risk for infertility (25).

456 In summary, this study demonstrates that endometrial Ct infection induces a miRNA-mediated
457 regulatory network that promotes EMT and alters immune cell balance, favoring Treg
458 differentiation over Th17 responses. These molecular changes likely contribute to tissue scarring
459 and impaired immune protection, offering new insights into the pathogenesis of Ct-induced
460 reproductive morbidity. Targeting these pathways may provide a foundation for innovative
461 therapeutic strategies to mitigate the long-term consequences of Ct infection.

462 **Disclosures**

463 The authors have no financial conflicts of interest.

464 **Acknowledgment**

465 We thank the women who agreed to participate in this study; Ingrid Macio, Melinda Petrina, Carol
466 Priest, Abi Jett, and Lorna Rabe, for their efforts in the clinic and the microbiology laboratory; and
467 the staff at the Allegheny County Health Department STD Clinic. We gratefully acknowledge the
468 technical support from the UNC High Throughput Sequencing Facility.

469 **Footnotes**

470 This work was supported by the National Institute of Allergy and Infectious Diseases
471 U19AI144181 and R01AI170959.

472

473

474

475

476 **References**

477 1. Chow, J. M., M. L. Yonekura, G. A. Richwald, S. Greenland, R. L. Sweet, and J.
478 Schachter. 1990. The association between Chlamydia trachomatis and ectopic pregnancy.
479 A matched-pair, case-control study. *JAMA* 263: 3164-3167.
480 2. Passos, L. G., P. Terraciano, N. Wolf, F. D. S. Oliveira, I. Almeida, and E. P. Passos.
481 2022. The Correlation between Chlamydia Trachomatis and Female Infertility: A
482 Systematic Review. *Rev Bras Ginecol Obstet* 44: 614-620.
483 3. Tang, W., J. Mao, K. T. Li, J. S. Walker, R. Chou, R. Fu, W. Chen, T. Darville, J.
484 Klausner, and J. D. Tucker. 2020. Pregnancy and fertility-related adverse outcomes
485 associated with Chlamydia trachomatis infection: a global systematic review and meta-
486 analysis. *Sex Transm Infect* 96: 322-329.
487 4. Huang, N., H. Chi, and J. Qiao. 2020. Role of Regulatory T Cells in Regulating Fetal-
488 Maternal Immune Tolerance in Healthy Pregnancies and Reproductive Diseases. *Front*
489 *Immunol* 11: 1023.
490 5. La Rocca, C., F. Carbone, S. Longobardi, and G. Matarese. 2014. The immunology of
491 pregnancy: regulatory T cells control maternal immune tolerance toward the fetus.
492 *Immunol Lett* 162: 41-48.
493 6. Stary, G., A. Olive, A. F. Radovic-Moreno, D. Gondek, D. Alvarez, P. A. Basto, M.
494 Perro, V. D. Vrbanac, A. M. Tager, J. Shi, J. A. Yethon, O. C. Farokhzad, R. Langer, M.
495 N. Starnbach, and U. H. von Andrian. 2015. VACCINES. A mucosal vaccine against
496 Chlamydia trachomatis generates two waves of protective memory T cells. *Science* 348:
497 aaa8205.
498 7. Yount, K. S., C. J. Chen, A. Kollipara, C. Liu, N. V. Mokashi, X. Zheng, C. B. Bagwell,
499 T. B. Poston, H. C. Wiesenfeld, S. L. Hillier, C. M. O'Connell, N. Stanley, and T.
500 Darville. 2024. Unique T cell signatures associated with reduced Chlamydia trachomatis
501 reinfection in a highly exposed cohort. *bioRxiv*.
502 8. Darville, T., and T. J. Hiltke. 2010. Pathogenesis of genital tract disease due to
503 Chlamydia trachomatis. *J Infect Dis* 201 Suppl 2: S114-125.
504 9. Rank, R. G., and J. A. Whittum-Hudson. 2010. Protective immunity to chlamydial genital
505 infection: evidence from animal studies. *J Infect Dis* 201 Suppl 2: S168-177.
506 10. Hart, K. M., A. J. Murphy, K. T. Barrett, C. R. Wira, P. M. Guyre, and P. A. Pioli. 2009.
507 Functional expression of pattern recognition receptors in tissues of the human female
508 reproductive tract. *J Reprod Immunol* 80: 33-40.
509 11. Darville, T., J. M. O'Neill, C. W. Andrews, Jr., U. M. Nagarajan, L. Stahl, and D. M.
510 Ojcius. 2003. Toll-like receptor-2, but not Toll-like receptor-4, is essential for
511 development of oviduct pathology in chlamydial genital tract infection. *J Immunol* 171:
512 6187-6197.
513 12. Frazer, L. C., C. M. O'Connell, C. W. Andrews, Jr., M. A. Zurenski, and T. Darville.
514 2011. Enhanced neutrophil longevity and recruitment contribute to the severity of oviduct
515 pathology during Chlamydia muridarum infection. *Infect Immun* 79: 4029-4041.
516 13. Lee, H. Y., J. H. Schripsema, I. M. Sigar, C. M. Murray, S. R. Lacy, and K. H. Ramsey.
517 2010. A link between neutrophils and chronic disease manifestations of Chlamydia
518 muridarum urogenital infection of mice. *FEMS Immunol Med Microbiol* 59: 108-116.

519 14. Rank, R. G., J. Whittimore, A. K. Bowlin, S. Dessus-Babus, and P. B. Wyrick. 2008.
520 Chlamydiae and polymorphonuclear leukocytes: unlikely allies in the spread of
521 chlamydial infection. *FEMS Immunol Med Microbiol* 54: 104-113.
522 15. Ramsey, K. H., I. M. Sigar, J. H. Schripsema, N. Shaba, and K. P. Cohoon. 2005.
523 Expression of matrix metalloproteinases subsequent to urogenital Chlamydia muridarum
524 infection of mice. *Infect Immun* 73: 6962-6973.
525 16. Murthy, A. K., W. Li, B. K. Chaganty, S. Kamalakaran, M. N. Guentzel, J. Seshu, T. G.
526 Forsthuber, G. Zhong, and B. P. Arulanandam. 2011. Tumor necrosis factor alpha
527 production from CD8+ T cells mediates oviduct pathological sequelae following primary
528 genital Chlamydia muridarum infection. *Infect Immun* 79: 2928-2935.
529 17. Gyorke, C. E., A. Kollipara, J. t. Allen, Y. Zhang, J. A. Ezzell, T. Darville, S. A.
530 Montgomery, and U. M. Nagarajan. 2020. IL-1alpha Is Essential for Oviduct Pathology
531 during Genital Chlamydial Infection in Mice. *J Immunol* 205: 3037-3049.
532 18. Igietseme, J. U., Y. Omosun, O. Stuchlik, M. S. Reed, J. Partin, Q. He, K. Joseph, D.
533 Ellerson, B. Bollweg, Z. George, F. O. Eko, C. Bandea, H. Liu, G. Yang, W. J. Shieh, J.
534 Pohl, K. Karem, and C. M. Black. 2015. Role of Epithelial-Mesenchyme Transition in
535 Chlamydia Pathogenesis. *PLoS One* 10: e0145198.
536 19. Igietseme, J. U., Y. Omosun, T. Nagy, O. Stuchlik, M. S. Reed, Q. He, J. Partin, K.
537 Joseph, D. Ellerson, Z. George, J. Goldstein, F. O. Eko, C. Bandea, J. Pohl, and C. M.
538 Black. 2018. Molecular Pathogenesis of Chlamydia Disease Complications: Epithelial-
539 Mesenchymal Transition and Fibrosis. *Infect Immun* 86.
540 20. Filipowicz, W., S. N. Bhattacharyya, and N. Sonenberg. 2008. Mechanisms of post-
541 transcriptional regulation by microRNAs: are the answers in sight? *Nat Rev Genet* 9: 102-
542 114.
543 21. O'Brien, J., H. Hayder, Y. Zayed, and C. Peng. 2018. Overview of MicroRNA
544 Biogenesis, Mechanisms of Actions, and Circulation. *Front Endocrinol (Lausanne)* 9:
545 402.
546 22. Lewis, B. P., I. H. Shih, M. W. Jones-Rhoades, D. P. Bartel, and C. B. Burge. 2003.
547 Prediction of mammalian microRNA targets. *Cell* 115: 787-798.
548 23. Dacco, M. D., M. Moustafa, D. Papoutsis, D. Georgantzis, G. Halmos, and A. Magos.
549 2012. An audit of using the H Pipelle for endometrial sampling at outpatient
550 hysteroscopy and literature review comparison with the Pipelle de Cornier. *Eur J Obstet*
551 *Gynecol Reprod Biol* 165: 299-301.
552 24. Kiviat, N. B., P. Wolner-Hanssen, D. A. Eschenbach, J. N. Wasserheit, J. A. Paavonen,
553 T. A. Bell, C. W. Critchlow, W. E. Stamm, D. E. Moore, and K. K. Holmes. 1990.
554 Endometrial histopathology in patients with culture-proved upper genital tract infection
555 and laparoscopically diagnosed acute salpingitis. *Am J Surg Pathol* 14: 167-175.
556 25. Wiesenfeld, H. C., S. L. Hillier, L. A. Meyn, A. J. Amortegui, and R. L. Sweet. 2012.
557 Subclinical pelvic inflammatory disease and infertility. *Obstet Gynecol* 120: 37-43.
558 26. Hunt, J. L., and A. A. Lynn. 2002. Histologic features of surgically removed fallopian
559 tubes. *Arch Pathol Lab Med* 126: 951-955.
560 27. Wiesenfeld, H. C., L. A. Meyn, T. Darville, I. S. Macio, and S. L. Hillier. 2021. A
561 Randomized Controlled Trial of Ceftriaxone and Doxycycline, With or Without
562 Metronidazole, for the Treatment of Acute Pelvic Inflammatory Disease. *Clin Infect Dis*
563 72: 1181-1189.

564 28. Workowski, K. A., G. A. Bolan, C. Centers for Disease, and Prevention. 2015. Sexually
565 transmitted diseases treatment guidelines, 2015. *MMWR Recomm Rep* 64: 1-137.
566 29. Russell, A. N., X. Zheng, C. M. O'Connell, B. D. Taylor, H. C. Wiesenfeld, S. L. Hillier,
567 W. Zhong, and T. Darville. 2016. Analysis of Factors Driving Incident and Ascending
568 Infection and the Role of Serum Antibody in Chlamydia trachomatis Genital Tract
569 Infection. *J Infect Dis* 213: 523-531.
570 30. Nugent, R. P., M. A. Krohn, and S. L. Hillier. 1991. Reliability of diagnosing bacterial
571 vaginosis is improved by a standardized method of gram stain interpretation. *J Clin*
572 *Microbiol* 29: 297-301.
573 31. Wiesenfeld, H. C., R. L. Sweet, R. B. Ness, M. A. Krohn, A. J. Amortegui, and S. L.
574 Hillier. 2005. Comparison of acute and subclinical pelvic inflammatory disease. *Sex*
575 *Transm Dis* 32: 400-405.
576 32. Zheng, X., C. M. O'Connell, W. Zhong, U. M. Nagarajan, M. Tripathy, D. Lee, A. N.
577 Russell, H. Wiesenfeld, S. Hillier, and T. Darville. 2018. Discovery of Blood
578 Transcriptional Endotypes in Women with Pelvic Inflammatory Disease. *J Immunol* 200:
579 2941-2956.
580 33. Zhang, Y., G. Parmigiani, and W. E. Johnson. 2020. ComBat-seq: batch effect
581 adjustment for RNA-seq count data. *NAR Genom Bioinform* 2: lqaa078.
582 34. Love, M. I., W. Huber, and S. Anders. 2014. Moderated estimation of fold change and
583 dispersion for RNA-seq data with DESeq2. *Genome Biol* 15: 550.
584 35. Gene Ontology, C., S. A. Aleksander, J. Balhoff, S. Carbon, J. M. Cherry, H. J. Drabkin,
585 D. Ebert, M. Feuermann, P. Gaudet, N. L. Harris, D. P. Hill, R. Lee, H. Mi, S. Moxon, C.
586 J. Mungall, A. Muruganugan, T. Mushayahama, P. W. Sternberg, P. D. Thomas, ..., and
587 M. Westerfield. 2023. The Gene Ontology knowledgebase in 2023. *Genetics* 224.
588 36. Rangel-Moreno, J., J. Moyron-Quiroz, K. Kusser, L. Hartson, H. Nakano, and T. D.
589 Randall. 2005. Role of CXC chemokine ligand 13, CC chemokine ligand (CCL) 19, and
590 CCL21 in the organization and function of nasal-associated lymphoid tissue. *J Immunol*
591 175: 4904-4913.
592 37. Carlsen, H. S., E. S. Baekkevold, F. E. Johansen, G. Haraldsen, and P. Brandtzaeg. 2002.
593 B cell attracting chemokine 1 (CXCL13) and its receptor CXCR5 are expressed in
594 normal and aberrant gut associated lymphoid tissue. *Gut* 51: 364-371.
595 38. Tolnay, M. 2022. Lymphocytes sense antibodies through human FCRL proteins:
596 Emerging roles in mucosal immunity. *J Leukoc Biol* 111: 477-487.
597 39. King, H. W., K. L. Wells, Z. Shipony, A. S. Kathiria, L. E. Wagar, C. Lareau, N. Orban,
598 R. Capasso, M. M. Davis, L. M. Steinmetz, L. K. James, and W. J. Greenleaf. 2021.
599 Integrated single-cell transcriptomics and epigenomics reveals strong germinal center-
600 associated etiology of autoimmune risk loci. *Sci Immunol* 6: eabh3768.
601 40. Wang, H., S. Jain, P. Li, J. X. Lin, J. Oh, C. Qi, Y. Gao, J. Sun, T. Sakai, Z. Naghashfar,
602 S. Abbasi, A. L. Kovalchuk, S. Bolland, S. L. Nutt, W. J. Leonard, and H. C. Morse, 3rd.
603 2019. Transcription factors IRF8 and PU.1 are required for follicular B cell development
604 and BCL6-driven germinal center responses. *Proc Natl Acad Sci U S A* 116: 9511-9520.
605 41. Di Ruocco, F., V. Basso, M. Rivoire, P. Mehlen, J. Ambati, S. De Falco, and V. Tarallo.
606 2018. Alu RNA accumulation induces epithelial-to-mesenchymal transition by
607 modulating miR-566 and is associated with cancer progression. *Oncogene* 37: 627-637.
608 42. Feng, J., S. Hu, K. Liu, G. Sun, and Y. Zhang. 2022. The Role of MicroRNA in the
609 Regulation of Tumor Epithelial-Mesenchymal Transition. *Cells* 11.

610 43. Wang, S., M. Zhang, T. Zhang, J. Deng, X. Xia, and X. Fang. 2020. microRNA-141
611 inhibits TGF-beta1-induced epithelial-to-mesenchymal transition through inhibition of
612 the TGF-beta1/SMAD2 signalling pathway in endometriosis. *Arch Gynecol Obstet* 301:
613 707-714.
614 44. Sun, Y., S. Shen, X. Liu, H. Tang, Z. Wang, Z. Yu, X. Li, and M. Wu. 2014. MiR-429
615 inhibits cells growth and invasion and regulates EMT-related marker genes by targeting
616 Onecut2 in colorectal carcinoma. *Mol Cell Biochem* 390: 19-30.
617 45. Zhang, L., Y. Chen, H. Wang, X. Zheng, C. Li, and Z. Han. 2018. miR-376a inhibits
618 breast cancer cell progression by targeting neuropilin-1 NR. *Onco Targets Ther* 11: 5293-
619 5302.
620 46. Lin, S., L. Tan, D. Luo, X. Peng, Y. Zhu, and H. Li. 2019. Linc01278 inhibits the
621 development of papillary thyroid carcinoma by regulating miR-376c-3p/DNM3 axis.
622 *Cancer Manag Res* 11: 8557-8569.
623 47. Zhao, X., X. Zhang, X. Zhang, T. Jiang, J. Zhai, H. Wang, M. Huang, R. Lang, and Q.
624 He. 2021. MiR-374b-5p inhibits KDM5B-induced epithelial-mesenchymal transition in
625 pancreatic cancer. *Am J Cancer Res* 11: 3907-3920.
626 48. Song, K., Y. Jiang, Y. Zhao, Y. Xie, J. Zhou, W. Yu, and Q. Wang. 2020. Members of
627 the miR-30 family inhibit the epithelial-to-mesenchymal transition of non-small-cell lung
628 cancer cells by suppressing XB130 expression levels. *Oncol Lett* 20: 68.
629 49. Lu, J., Z. Zhao, and Y. Ma. 2020. miR-186 Represses Proliferation, Migration, Invasion,
630 and EMT of Hepatocellular Carcinoma via Directly Targeting CDK6. *Oncol Res* 28: 509-
631 518.
632 50. Tian, X., Q. Fei, M. Du, H. Zhu, J. Ye, L. Qian, Z. Lu, W. Zhang, Y. Wang, F. Peng, J.
633 Chen, B. Liu, Q. Li, X. He, and L. Yin. 2019. miR-130a-3p regulated TGF-beta1-induced
634 epithelial-mesenchymal transition depends on SMAD4 in EC-1 cells. *Cancer Med* 8:
635 1197-1208.
636 51. Du, W., H. Tang, Z. Lei, J. Zhu, Y. Zeng, Z. Liu, and J. A. Huang. 2019. miR-335-5p
637 inhibits TGF-beta1-induced epithelial-mesenchymal transition in non-small cell lung
638 cancer via ROCK1. *Respir Res* 20: 225.
639 52. Fang, L. L., X. H. Wang, B. F. Sun, X. D. Zhang, X. H. Zhu, Z. J. Yu, and H. Luo. 2017.
640 Expression, regulation and mechanism of action of the miR-17-92 cluster in tumor cells
641 (Review). *Int J Mol Med* 40: 1624-1630.
642 53. Qi, J. C., Z. Yang, Y. P. Zhang, B. S. Lu, Y. W. Yin, K. L. Liu, W. Y. Xue, C. B. Qu, and
643 W. Li. 2019. miR-20b-5p, TGFBR2, and E2F1 Form a Regulatory Loop to Participate in
644 Epithelial to Mesenchymal Transition in Prostate Cancer. *Front Oncol* 9: 1535.
645 54. Khalilian, S., H. Abedinlou, B. M. Hussen, S. Z. H. Imani, and S. Ghafouri-Fard. 2022.
646 The emerging role of miR-20b in human cancer and other disorders: Pathophysiology and
647 therapeutic implications. *Front Oncol* 12: 985457.
648 55. Morizane, R., S. Fujii, T. Monkawa, K. Hiratsuka, S. Yamaguchi, K. Homma, and H.
649 Itoh. 2014. miR-34c attenuates epithelial-mesenchymal transition and kidney fibrosis
650 with ureteral obstruction. *Sci Rep* 4: 4578.
651 56. Li, C., J. Xia, W. Yao, G. Yang, Y. Tian, Y. Qi, and C. Hao. 2022. Mechanism of
652 LncRNA XIST/ miR-101-3p/ZEB1 axis in EMT associated with silicosis. *Toxicol Lett*
653 360: 11-19.

654 57. Dong, P., M. Kaneuchi, H. Watari, J. Hamada, S. Sudo, J. Ju, and N. Sakuragi. 2011.
655 MicroRNA-194 inhibits epithelial to mesenchymal transition of endometrial cancer cells
656 by targeting oncogene BMI-1. *Mol Cancer* 10: 99.
657 58. Chen, J., S. Gao, C. Wang, Z. Wang, H. Zhang, K. Huang, B. Zhou, H. Li, Z. Yu, J. Wu,
658 and C. Chen. 2016. Pathologically decreased expression of miR-193a contributes to
659 metastasis by targeting WT1-E-cadherin axis in non-small cell lung cancers. *J Exp Clin*
660 *Cancer Res* 35: 173.
661 59. Li, J., Y. Song, Y. Wang, J. Luo, and W. Yu. 2013. MicroRNA-148a suppresses
662 epithelial-to-mesenchymal transition by targeting ROCK1 in non-small cell lung cancer
663 cells. *Mol Cell Biochem* 380: 277-282.
664 60. Hu, B., Z. Chen, X. Wang, F. Chen, Z. Song, and C. Cao. 2021. MicroRNA-148a-3p
665 Directly Targets SERPINE1 to Suppress EMT-Mediated Colon Adenocarcinoma
666 Progression. *Cancer Manag Res* 13: 6349-6362.
667 61. Miscianinov, V., A. Martello, L. Rose, E. Parish, B. Cathcart, T. Mitic, G. A. Gray, M.
668 Meloni, A. Al Haj Zen, and A. Caporali. 2018. MicroRNA-148b Targets the TGF-beta
669 Pathway to Regulate Angiogenesis and Endothelial-to-Mesenchymal Transition during
670 Skin Wound Healing. *Mol Ther* 26: 1996-2007.
671 62. Jia, Z., Y. Zhang, Q. Xu, W. Guo, and A. Guo. 2018. miR-126 suppresses epithelial-to-
672 mesenchymal transition and metastasis by targeting PI3K/AKT/Snail signaling of lung
673 cancer cells. *Oncol Lett* 15: 7369-7375.
674 63. Jiang, R., C. Zhang, G. Liu, R. Gu, and H. Wu. 2017. MicroRNA-126 Inhibits
675 Proliferation, Migration, Invasion, and EMT in Osteosarcoma by Targeting ZEB1. *J Cell*
676 *Biochem* 118: 3765-3774.
677 64. Yao, Y., Q. Xu, L. Yan, Y. Jiao, Q. Su, X. Li, C. Liu, and F. Zhao. 2020. MiRNA-128
678 and MiRNA-142 Regulate Tumorigenesis and EMT in Oral Squamous Cell Carcinoma
679 Through HOXA10. *Cancer Manag Res* 12: 9987-9997.
680 65. Pao, S. I., L. T. Lin, Y. H. Chen, C. L. Chen, and J. T. Chen. 2021. Repression of Smad4
681 by MicroRNA-1285 moderates TGF-beta-induced epithelial-mesenchymal transition in
682 proliferative vitreoretinopathy. *PLoS One* 16: e0254873.
683 66. Jiang, M., L. Shi, C. Yang, Y. Ge, L. Lin, H. Fan, Y. He, D. Zhang, Y. Miao, and L.
684 Yang. 2019. miR-1254 inhibits cell proliferation, migration, and invasion by down-
685 regulating Smurf1 in gastric cancer. *Cell Death Dis* 10: 32.
686 67. Yan, S., M. Cheng, Q. Duan, Z. Wang, W. Gao, B. Ren, and D. Xu. 2019. MiR-6803-5p
687 Promotes Cancer Cell Proliferation and Invasion via PTPRO/NF-kappaB Axis in
688 Colorectal Cancer. *Mediators Inflamm* 2019: 8128501.
689 68. Zhu, X., S. Ju, F. Yuan, G. Chen, Y. Shu, C. Li, Y. Xu, J. Luo, and L. Xia. 2017.
690 microRNA-664 enhances proliferation, migration and invasion of lung cancer cells. *Exp*
691 *Ther Med* 13: 3555-3562.
692 69. You, X., Y. Wang, J. Meng, S. Han, L. Liu, Y. Sun, J. Zhang, S. Sun, X. Li, W. Sun, Y.
693 Dong, and Y. Zhang. 2021. Exosomal miR-663b exposed to TGF-beta1 promotes
694 cervical cancer metastasis and epithelial-mesenchymal transition by targeting MGAT3.
695 *Oncol Rep* 45.
696 70. Hamada, S., K. Satoh, S. Miura, M. Hirota, A. Kanno, A. Masamune, K. Kikuta, K.
697 Kume, J. Unno, S. Egawa, F. Motoi, M. Unno, and T. Shimosegawa. 2013. miR-197
698 induces epithelial-mesenchymal transition in pancreatic cancer cells by targeting p120
699 catenin. *J Cell Physiol* 228: 1255-1263.

700 71. Miao, L. J., S. Yan, Q. F. Zhuang, Q. Y. Mao, D. Xue, X. Z. He, and J. P. Chen. 2019.
701 miR-106b promotes proliferation and invasion by targeting Capicua through MAPK
702 signaling in renal carcinoma cancer. *Onco Targets Ther* 12: 3595-3607.
703 72. Luan, W., Y. Ding, H. Xi, H. Ruan, F. Lu, S. Ma, and J. Wang. 2021. Exosomal miR-
704 106b-5p derived from melanoma cell promotes primary melanocytes epithelial-
705 mesenchymal transition through targeting EphA4. *J Exp Clin Cancer Res* 40: 107.
706 73. Yang, C., R. Dou, C. Wei, K. Liu, D. Shi, C. Zhang, Q. Liu, S. Wang, and B. Xiong.
707 2021. Tumor-derived exosomal microRNA-106b-5p activates EMT-cancer cell and M2-
708 subtype TAM interaction to facilitate CRC metastasis. *Mol Ther* 29: 2088-2107.
709 74. Wang, S., X. Zhang, C. Yang, and S. Xu. 2019. MicroRNA-198-5p inhibits the migration
710 and invasion of non-small lung cancer cells by targeting fucosyltransferase 8. *Clin Exp*
711 *Pharmacol Physiol* 46: 955-967.
712 75. Wang, H., D. Kanmangne, R. Li, Z. Qian, X. Xia, X. Wang, and T. Wang. 2020.
713 miR-30a-3p suppresses the proliferation and migration of lung adenocarcinoma cells by
714 downregulating CNPY2. *Oncol Rep* 43: 646-654.
715 76. Wang, X., J. Wang, G. Huang, Y. Li, and S. Guo. 2021. miR-320a-3P alleviates the
716 epithelial-mesenchymal transition of A549 cells by activation of STAT3/SMAD3
717 signaling in a pulmonary fibrosis model. *Mol Med Rep* 23.
718 77. Liu, X., J. Song, Y. Kang, Y. Wang, and A. Chen. 2022. CircPDSS1 promotes the
719 proliferation, invasion, migration, and EMT of breast cancer cell via regulating miR-
720 320c/CKAP5 axis. *Cancer Cell Int* 22: 238.
721 78. Shi, S., X. Hu, J. Xu, H. Liu, and L. Zou. 2018. MiR-320d suppresses the progression of
722 breast cancer via lncRNA HNF1A-AS1 regulation and SOX4 inhibition. *RSC Adv* 8:
723 19196-19207.
724 79. Hou, B., H. Ishinaga, K. Midorikawa, S. Nakamura, Y. Hiraku, S. Oikawa, N. Ma, K.
725 Takeuchi, and M. Murata. 2018. Let-7c inhibits migration and epithelial-mesenchymal
726 transition in head and neck squamous cell carcinoma by targeting IGF1R and HMGA2.
727 *Oncotarget* 9: 8927-8940.
728 80. Liang, L., Y. W. Zheng, and Y. L. Wang. 2020. miR-4429 Regulates the Proliferation,
729 Migration, Invasion, and Epithelial-Mesenchymal Transition of Cervical Cancer by
730 Targeting FOXM1. *Cancer Manag Res* 12: 5301-5312.
731 81. Pan, H., Y. Hong, B. Yu, L. Li, and X. Zhang. 2019. miR-4429 Inhibits Tumor
732 Progression and Epithelial-Mesenchymal Transition Via Targeting CDK6 in Clear Cell
733 Renal Cell Carcinoma. *Cancer Biother Radiopharm* 34: 334-341.
734 82. Dong, P., M. Karaayvaz, N. Jia, M. Kaneuchi, J. Hamada, H. Watari, S. Sudo, J. Ju, and
735 N. Sakuragi. 2013. Mutant p53 gain-of-function induces epithelial-mesenchymal
736 transition through modulation of the miR-130b-ZEB1 axis. *Oncogene* 32: 3286-3295.
737 83. Li, B. L., C. Lu, W. Lu, T. T. Yang, J. Qu, X. Hong, and X. P. Wan. 2013. miR-130b is
738 an EMT-related microRNA that targets DICER1 for aggression in endometrial cancer.
739 *Med Oncol* 30: 484.
740 84. Chang, R. M., J. F. Xu, F. Fang, H. Yang, and L. Y. Yang. 2016. MicroRNA-130b
741 promotes proliferation and EMT-induced metastasis via PTEN/p-AKT/HIF-1alpha
742 signaling. *Tumour Biol* 37: 10609-10619.
743 85. Arisan, E. D., O. Rencuzogullari, C. Cieza-Borrella, F. Miralles Arenas, M. Dwek, S.
744 Lange, and P. Uysal-Onganer. 2021. MiR-21 Is Required for the Epithelial-Mesenchymal
745 Transition in MDA-MB-231 Breast Cancer Cells. *Int J Mol Sci* 22.

746 86. Ghosh, A., N. Ranjan, L. Jiang, A. H. Ansari, N. Degyatoreva, S. Ahluwalia, D. P. Arya,
747 and S. Maiti. 2022. Fine-tuning miR-21 expression and inhibition of EMT in breast
748 cancer cells using aromatic-neomycin derivatives. *Mol Ther Nucleic Acids* 27: 685-698.
749 87. Zhao, N., H. Sun, B. Sun, D. Zhu, X. Zhao, Y. Wang, Q. Gu, X. Dong, F. Liu, Y. Zhang,
750 and X. Li. 2016. miR-27a-3p suppresses tumor metastasis and VM by down-regulating
751 VE-cadherin expression and inhibiting EMT: an essential role for Twist-1 in HCC. *Sci*
752 *Rep* 6: 23091.
753 88. Pan, G., Y. Liu, L. Shang, F. Zhou, and S. Yang. 2021. EMT-associated microRNAs and
754 their roles in cancer stemness and drug resistance. *Cancer Commun (Lond)* 41: 199-217.
755 89. Zhang, J., X. Hua, N. Qi, G. Han, J. Yu, Y. Yu, X. Wei, H. Li, X. Chen, C. Leng, Q. Liu,
756 Y. Lu, and Y. Li. 2020. MiR-27b suppresses epithelial-mesenchymal transition and
757 chemoresistance in lung cancer by targeting Snail1. *Life Sci* 254: 117238.
758 90. Suzuki, H. I., A. Katsura, H. Mihira, M. Horie, A. Saito, and K. Miyazono. 2017.
759 Regulation of TGF-beta-mediated endothelial-mesenchymal transition by microRNA-27.
760 *J Biochem* 161: 417-420.
761 91. Lu, Y., W. Huang, H. Chen, H. Wei, A. Luo, G. Xia, X. Deng, and G. Zhang. 2019.
762 MicroRNA-224, negatively regulated by c-jun, inhibits growth and epithelial-to-
763 mesenchymal transition phenotype via targeting ADAM17 in oral squamous cell
764 carcinoma. *J Cell Mol Med* 23: 4913-4920.
765 92. Zang, C. S., H. T. Huang, J. Qiu, J. Sun, R. F. Ge, and L. W. Jiang. 2020. MiR-224-5p
766 targets EGR2 to promote the development of papillary thyroid carcinoma. *Eur Rev Med*
767 *Pharmacol Sci* 24: 4890-4900.
768 93. Hsiao, S. Y., S. M. Weng, J. R. Hsiao, Y. Y. Wu, J. E. Wu, C. H. Tung, W. L. Shen, S. F.
769 Sun, W. T. Huang, C. Y. Lin, S. H. Chen, T. M. Hong, Y. L. Chen, and J. Y. Chang.
770 2023. MiR-455-5p suppresses PDZK1IP1 to promote the motility of oral squamous cell
771 carcinoma and accelerate clinical cancer invasion by regulating partial epithelial-to-
772 mesenchymal transition. *J Exp Clin Cancer Res* 42: 40.
773 94. Meng, C., K. Liu, X. Cai, and Y. Chen. 2021. Mechanism of miR-455-3 in suppressing
774 epithelial-mesenchymal transition and angiogenesis of non-small cell lung cancer cells.
775 *Cell Stress Chaperones* 27: 107-117.
776 95. Chen, Y., D. Sun, D. Shang, Z. Jiang, P. Miao, and J. Gao. 2022. miR-223-3p alleviates
777 TGF-beta-induced epithelial-mesenchymal transition and extracellular matrix deposition
778 by targeting SP3 in endometrial epithelial cells. *Open Med (Wars)* 17: 518-526.
779 96. Ke, Y., W. Zhao, J. Xiong, and R. Cao. 2013. miR-149 Inhibits Non-Small-Cell Lung
780 Cancer Cells EMT by Targeting FOXM1. *Biochem Res Int* 2013: 506731.
781 97. Wang, J., and L. Liu. 2021. MiR-149-3p promotes the cisplatin resistance and EMT in
782 ovarian cancer through downregulating TIMP2 and CDKN1A. *J Ovarian Res* 14: 165.
783 98. Sun, Y., Y. Yi, S. Gan, R. Ye, C. Huang, M. Li, J. Huang, and Y. Guo. 2021. miR-574-5p
784 mediates epithelial-mesenchymal transition in small cell lung cancer by targeting
785 vimentin via a competitive endogenous RNA network. *Oncol Lett* 21: 459.
786 99. Zhang, K. J., Y. Hu, N. Luo, X. Li, F. Y. Chen, J. Q. Yuan, and L. Guo. 2020.
787 miR-574-5p attenuates proliferation, migration and EMT in triple-negative breast cancer
788 cells by targeting BCL11A and SOX2 to inhibit the SKIL/TAZ/CTGF axis. *Int J Oncol*
789 56: 1240-1251.
790 100. Wang, C., W. Zhang, L. Zhang, X. Chen, F. Liu, J. Zhang, S. Guan, Y. Sun, P. Chen, D.
791 Wang, E. Un Nesa, Y. Cheng, and G. M. Yousef. 2016. miR-146a-5p mediates epithelial-

792 mesenchymal transition of oesophageal squamous cell carcinoma via targeting Notch2.
793 *Br J Cancer* 115: 1548-1554.
794 101. Wang, F., L. J. Ye, F. J. Wang, H. F. Liu, and X. L. Wang. 2020. miR-146a promotes
795 proliferation, invasion, and epithelial-to-mesenchymal transition in oral squamous
796 carcinoma cells. *Environ Toxicol* 35: 1050-1057.
797 102. Liang, Y., S. Li, and L. Tang. 2021. MicroRNA 320, an Anti-Oncogene Target miRNA
798 for Cancer Therapy. *Biomedicines* 9.
799 103. Liu, R. Y., Y. Zeng, Z. Lei, L. Wang, H. Yang, Z. Liu, J. Zhao, and H. T. Zhang. 2014.
800 JAK/STAT3 signaling is required for TGF-beta-induced epithelial-mesenchymal
801 transition in lung cancer cells. *Int J Oncol* 44: 1643-1651.
802 104. Gregory, P. A., C. P. Bracken, E. Smith, A. G. Bert, J. A. Wright, S. Roslan, M. Morris,
803 L. Wyatt, G. Farshid, Y. Y. Lim, G. J. Lindeman, M. F. Shannon, P. A. Drew, Y. Khew-
804 Goodall, and G. J. Goodall. 2011. An autocrine TGF-beta/ZEB/miR-200 signaling
805 network regulates establishment and maintenance of epithelial-mesenchymal transition.
806 *Mol Biol Cell* 22: 1686-1698.
807 105. Bettelli, E., Y. Carrier, W. Gao, T. Korn, T. B. Strom, M. Oukka, H. L. Weiner, and V.
808 K. Kuchroo. 2006. Reciprocal developmental pathways for the generation of pathogenic
809 effector TH17 and regulatory T cells. *Nature* 441: 235-238.
810 106. Guan, T., C. X. Dominguez, R. A. Amezquita, B. J. Laidlaw, J. Cheng, J. Henao-Mejia,
811 A. Williams, R. A. Flavell, J. Lu, and S. M. Kaech. 2018. ZEB1, ZEB2, and the miR-200
812 family form a counterregulatory network to regulate CD8(+) T cell fates. *J Exp Med* 215:
813 1153-1168.
814 107. Wang, X. Y., X. Y. Chen, J. Li, H. Y. Zhang, J. Liu, and L. D. Sun. 2017. MiR-200a
815 expression in CD4+ T cells correlates with the expression of Th17/Treg cells and relevant
816 cytokines in psoriasis vulgaris: A case control study. *Biomed Pharmacother* 93: 1158-
817 1164.
818 108. Naghavian, R., K. Ghaedi, A. Kiani-Esfahani, M. Ganjalikhani-Hakemi, M. Etemadifar,
819 and M. H. Nasr-Esfahani. 2015. miR-141 and miR-200a, Revelation of New Possible
820 Players in Modulation of Th17/Treg Differentiation and Pathogenesis of Multiple
821 Sclerosis. *PLoS One* 10: e0124555.
822 109. Bahmani, L., M. Baghi, M. Peymani, A. Javeri, and K. Ghaedi. 2021. MiR-141-3p and
823 miR-200a-3p are involved in Th17 cell differentiation by negatively regulating RARB
824 expression. *Hum Cell* 34: 1375-1387.
825 110. Yu, X., X. Fan, X. Zhang, P. Wei, H. Zhou, D. Liu, and B. Chen. 2023. miR-429 inhibits
826 the formation of an immunosuppressive microenvironment to counteract hepatocellular
827 carcinoma immune escape by targeting PD-L1. *Funct Integr Genomics* 23: 312.
828 111. Jebbawi, F., H. Fayyad-Kazan, M. Merimi, P. Lewalle, J. C. Verougstraete, O. Leo, P.
829 Romero, A. Burny, B. Badran, P. Martiat, and R. Rouas. 2014. A microRNA profile of
830 human CD8(+) regulatory T cells and characterization of the effects of microRNAs on
831 Treg cell-associated genes. *J Transl Med* 12: 218.
832 112. Cruz, L. O., S. S. Hashemifar, C. J. Wu, S. Cho, D. T. Nguyen, L. L. Lin, A. A. Khan,
833 and L. F. Lu. 2017. Excessive expression of miR-27 impairs Treg-mediated
834 immunological tolerance. *J Clin Invest* 127: 530-542.
835 113. Zhou, Y., Y. Li, J. Lu, X. Hong, and L. Xu. 2019. MicroRNA-30a controls the instability
836 of inducible CD4+ Tregs through SOCS1. *Mol Med Rep* 20: 4303-4314.

114. Li, J. Q., J. M. Tian, X. R. Fan, Z. Y. Wang, J. Ling, X. F. Wu, F. Y. Yang, and Y. L. Xia. 2020. miR-106b-5p induces immune imbalance of Treg/Th17 in immune thrombocytopenic purpura through NR4A3/Foxp3 pathway. *Cell Cycle* 19: 1265-1274.
115. Jiao, P., X. P. Wang, Z. M. Luoreng, J. Yang, L. Jia, Y. Ma, and D. W. Wei. 2021. miR-223: An Effective Regulator of Immune Cell Differentiation and Inflammation. *Int J Biol Sci* 17: 2308-2322.
116. Chang, C. C., Q. Y. Zhang, Z. Liu, R. A. Clynes, N. Suciu-Foca, and G. Vlad. 2012. Downregulation of inflammatory microRNAs by Ig-like transcript 3 is essential for the differentiation of human CD8(+) T suppressor cells. *J Immunol* 188: 3042-3052.
117. Lu, L. F., M. P. Boldin, A. Chaudhry, L. L. Lin, K. D. Taganov, T. Hanada, A. Yoshimura, D. Baltimore, and A. Y. Rudensky. 2010. Function of miR-146a in controlling Treg cell-mediated regulation of Th1 responses. *Cell* 142: 914-929.
118. Zhou, Q., S. Haupt, J. T. Kreuzer, A. Hammitzsch, F. Proft, C. Neumann, J. Leipe, M. Witt, H. Schulze-Koops, and A. Skapenko. 2015. Decreased expression of miR-146a and miR-155 contributes to an abnormal Treg phenotype in patients with rheumatoid arthritis. *Ann Rheum Dis* 74: 1265-1274.
119. Li, C., P. J. Ebert, and Q. J. Li. 2013. T cell receptor (TCR) and transforming growth factor beta (TGF-beta) signaling converge on DNA (cytosine-5)-methyltransferase to control forkhead box protein 3 (foxp3) locus methylation and inducible regulatory T cell differentiation. *J Biol Chem* 288: 19127-19139.
120. Yang, H. Y., J. Barbi, C. Y. Wu, Y. Zheng, P. D. Vignali, X. Wu, J. H. Tao, B. V. Park, S. Bandara, L. Novack, X. Ni, X. Yang, K. Y. Chang, R. C. Wu, J. Zhang, C. W. Yang, D. M. Pardoll, H. Li, and F. Pan. 2016. MicroRNA-17 Modulates Regulatory T Cell Function by Targeting Co-regulators of the Foxp3 Transcription Factor. *Immunity* 45: 83-93.
121. de Kouchkovsky, D., J. H. Esensten, W. L. Rosenthal, M. M. Morar, J. A. Bluestone, and L. T. Jeker. 2013. microRNA-17-92 regulates IL-10 production by regulatory T cells and control of experimental autoimmune encephalomyelitis. *J Immunol* 191: 1594-1605.
122. Skinner, J. P., A. A. Keown, and M. M. Chong. 2014. The miR-17 approximately 92a cluster of microRNAs is required for the fitness of Foxp3+ regulatory T cells. *PLoS One* 9: e88997.
123. Dong, L., X. Wang, J. Tan, H. Li, W. Qian, J. Chen, Q. Chen, J. Wang, W. Xu, C. Tao, and S. Wang. 2014. Decreased expression of microRNA-21 correlates with the imbalance of Th17 and Treg cells in patients with rheumatoid arthritis. *J Cell Mol Med* 18: 2213-2224.
124. Li, D., X. Du, M. Zhu, S. Yang, and W. Zhao. 2020. MiR-374b-5p Regulates T Cell Differentiation and Is Associated with rEg.P29 Immunity. *Biomed Res Int* 2020: 8024763.
125. Sun, R., P. P. Zhang, X. Q. Weng, X. D. Gao, C. X. Huang, L. Wang, X. X. Hu, P. P. Xu, L. Cheng, L. Jiang, D. Fu, B. Qu, Y. Zhao, Y. Feng, H. J. Dou, Z. Zheng, and W. L. Zhao. 2022. Therapeutic targeting miR130b counteracts diffuse large B-cell lymphoma progression via OX40/OX40L-mediated interaction with Th17 cells. *Signal Transduct Target Ther* 7: 80.
126. Liu, S. Q., S. Jiang, C. Li, B. Zhang, and Q. J. Li. 2014. miR-17-92 cluster targets phosphatase and tensin homology and Ikaros Family Zinc Finger 4 to promote TH17-mediated inflammation. *J Biol Chem* 289: 12446-12456.

127. Honardoost, M. A., R. Naghavian, F. Ahmadinejad, A. Hosseini, and K. Ghaedi. 2015. Integrative computational mRNA-miRNA interaction analyses of the autoimmune-deregulated miRNAs and well-known Th17 differentiation regulators: An attempt to discover new potential miRNAs involved in Th17 differentiation. *Gene* 572: 153-162.
128. Wei, Y., S. Chen, D. Sun, X. Li, R. Wei, X. Li, and H. Nian. 2019. miR-223-3p promotes autoreactive T(h)17 cell responses in experimental autoimmune uveitis (EAU) by inhibiting transcription factor FOXO3 expression. *FASEB J* 33: 13951-13965.
129. Angelou, C. C., A. C. Wells, J. Vijayaraghavan, C. E. Dougan, R. Lawlor, E. Iverson, V. Lazarevic, M. Y. Kimura, S. R. Peyton, L. M. Minter, B. A. Osborne, E. L. Pobezinskaya, and L. A. Pobezinsky. 2019. Differentiation of Pathogenic Th17 Cells Is Negatively Regulated by Let-7 MicroRNAs in a Mouse Model of Multiple Sclerosis. *Front Immunol* 10: 3125.
130. Qu, X., J. Zhou, T. Wang, J. Han, L. Ma, H. Yu, D. Geng, H. Fan, Q. Zhang, F. Hua, and R. Yao. 2016. MiR-30a inhibits Th17 differentiation and demyelination of EAE mice by targeting the IL-21R. *Brain Behav Immun* 57: 193-199.
131. Zhu, E., X. Wang, B. Zheng, Q. Wang, J. Hao, S. Chen, Q. Zhao, L. Zhao, Z. Wu, and Z. Yin. 2014. miR-20b suppresses Th17 differentiation and the pathogenesis of experimental autoimmune encephalomyelitis by targeting RORgammat and STAT3. *J Immunol* 192: 5599-5609.
132. Chen, J., X. Shi, Y. Deng, J. Dang, Y. Liu, J. Zhao, R. Liang, D. Zeng, W. Wu, Y. Xiong, J. Yuan, Y. Chen, J. Wang, W. Lin, X. Chen, W. Huang, N. Olsen, Y. Pan, Q. Fu, and S. G. Zheng. 2024. miRNA-148a-containing GMSC-derived EVs modulate Treg/Th17 balance via IKKB/NF-kappaB pathway and treat a rheumatoid arthritis model. *JCI Insight* 9.
133. Pacholewska, A., M. F. Kraft, V. Gerber, and V. Jagannathan. 2017. Differential Expression of Serum MicroRNAs Supports CD4(+) T Cell Differentiation into Th2/Th17 Cells in Severe Equine Asthma. *Genes (Basel)* 8.
134. Cao, Y., Z. Wang, Y. Yan, L. Ji, J. He, B. Xuan, C. Shen, Y. Ma, S. Jiang, D. Ma, T. Tong, X. Zhang, Z. Gao, X. Zhu, J. Y. Fang, H. Chen, and J. Hong. 2021. Enterotoxigenic Bacteroidesfragilis Promotes Intestinal Inflammation and Malignancy by Inhibiting Exosome-Packaged miR-149-3p. *Gastroenterology* 161: 1552-1566 e1512.
135. Ahmadian-Elmi, M., A. Bidmeshki Pour, R. Naghavian, K. Ghaedi, S. Tanhaei, T. Izadi, and M. H. Nasr-Esfahani. 2016. miR-27a and miR-214 exert opposite regulatory roles in Th17 differentiation via mediating different signaling pathways in peripheral blood CD4+ T lymphocytes of patients with relapsing-remitting multiple sclerosis. *Immunogenetics* 68: 43-54.
136. Cho, S., C. J. Wu, T. Yasuda, L. O. Cruz, A. A. Khan, L. L. Lin, D. T. Nguyen, M. Miller, H. M. Lee, M. L. Kuo, D. H. Broide, K. Rajewsky, A. Y. Rudensky, and L. F. Lu. 2016. miR-23 approximately 27 approximately 24 clusters control effector T cell differentiation and function. *J Exp Med* 213: 235-249.
137. Akimniyazova, A., A. Pyrkova, V. Uversky, and A. Ivashchenko. 2021. Predicting Associations of miRNAs and Candidate Gastric Cancer Genes for Nanomedicine. *Nanomaterials (Basel)* 11.
138. Hironaka-Mitsuhashi, A., K. Otsuka, L. Gailhouste, A. Sanchez Calle, M. Kumazaki, Y. Yamamoto, Y. Fujiwara, and T. Ochiya. 2020. MiR-1285-5p/TMEM194A axis affects cell proliferation in breast cancer. *Cancer Sci* 111: 395-405.

139. Zhang, J., X. Li, J. Yang, and Y. Zhang. 2022. MiR-1254 suppresses the proliferation and invasion of cervical cancer cells by modulating CD36. *J Transl Med* 19: 531.
140. Zhao, M. C., M. M. Zhang, T. Li, Z. H. Tao, Y. Q. Du, L. P. Wang, J. Zhang, B. Y. Wang, and X. C. Hu. 2020. MiR-566 protects the malignant progression of breast cancer by negatively regulating WNT6. *Eur Rev Med Pharmacol Sci* 24: 6185-6194.
141. Zhou, J., M. Zhang, Y. Huang, L. Feng, H. Chen, Y. Hu, H. Chen, K. Zhang, L. Zheng, and S. Zheng. 2015. MicroRNA-320b promotes colorectal cancer proliferation and invasion by competing with its homologous microRNA-320a. *Cancer Lett* 356: 669-675.
142. Pastor-Fernandez, G., I. R. Mariblanca, and M. N. Navarro. 2020. Decoding IL-23 Signaling Cascade for New Therapeutic Opportunities. *Cells* 9.
143. Yeruva, L., D. L. Pouncey, M. R. Eledge, S. Bhattacharya, C. Luo, E. W. Weatherford, D. M. Ojcius, and R. G. Rank. 2017. MicroRNAs Modulate Pathogenesis Resulting from Chlamydial Infection in Mice. *Infect Immun* 85.
144. Yeruva, L., A. K. Bowlin, N. Spencer, A. T. Maurelli, and R. G. Rank. 2015. Chlamydial variants differ in ability to ascend the genital tract in the guinea pig model of chlamydial genital infection. *Infect Immun* 83: 3176-3183.
145. Rajeeve, K., S. Das, B. K. Prusty, and T. Rudel. 2018. Chlamydia trachomatis paralyses neutrophils to evade the host innate immune response. *Nat Microbiol* 3: 824-835.

975 **Figures**

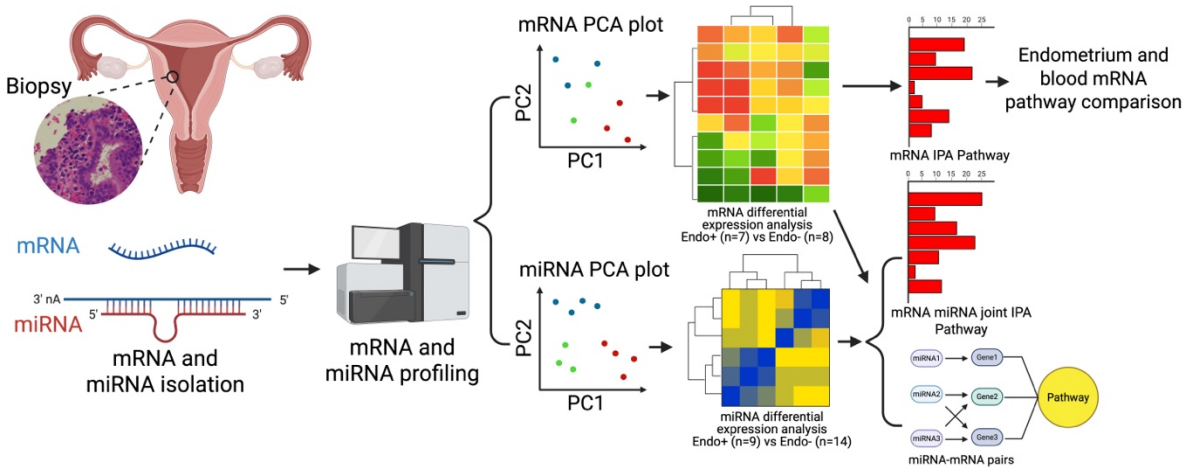

976
977 **Figure 1. Workflow depicting sample processing, mRNA and miRNA profiling and**
978 **subsequent analytical methods.** Endometrial biopsy samples were processed to profile mRNA
979 from 7 Endo (+) and 8 Endo (-) women, including 4 cervix (+) only and 4 uninfected, and
980 miRNA from 9 Endo (+) and 14 Endo (-) women, including 5 cervix(+) only and 9 uninfected.
981 Relationships among cohort participants based on their transcriptomes were revealed by
982 Principal Component Analysis (PCA). Differentially expressed (DE) mRNAs and miRNAs
983 between Endo+ and Endo- biopsies were determined and functional annotation of DE mRNA
984 and miRNA-mRNA pairs were provided by IPA. Additionally, endometrial biopsy generated
985 mRNA data were compared to previously published blood mRNA data generated from
986 participants in the T Cell Response Against Chlamydia (TRAC) cohort (32).
987

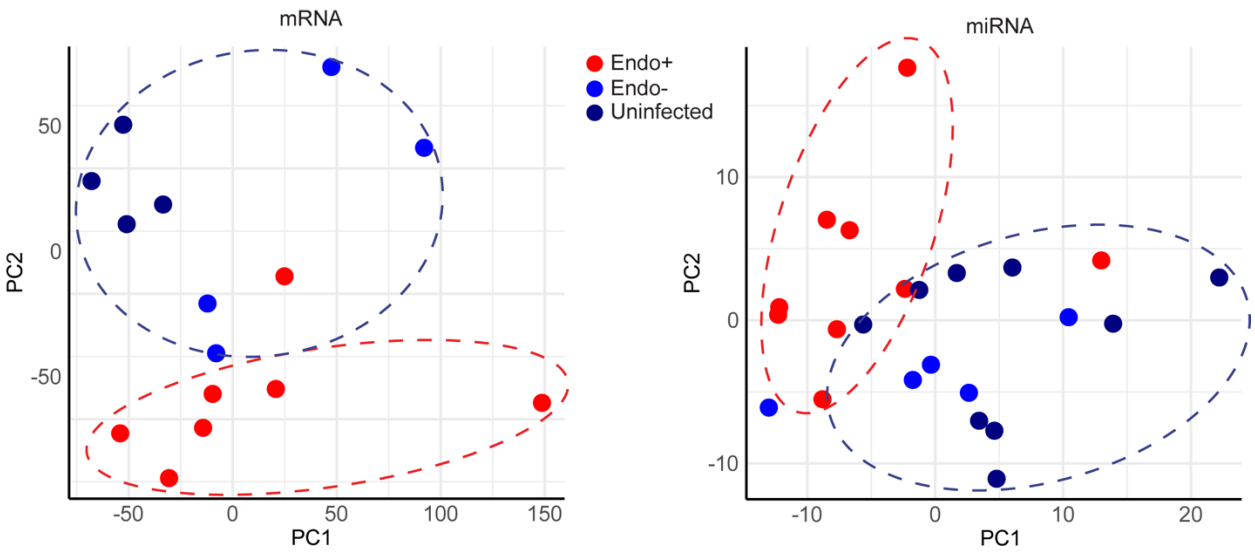

Figure 2. Principal component analysis (PCA) of endometrial transcriptome (A) mRNA and (B) miRNA. Each dot represents one subject, with infection status indicated by color. Red denotes endometrial infection (Endo+), light blue denotes absence of endometrial infection but positive cervical infection (Endo-), and dark blue (Uninfected). The x-axis represents the first principal component, PC1, which accounts for the largest variance of mRNA (A) or miRNA (B) expression, and the y axis, PC2, explains the second largest variance.

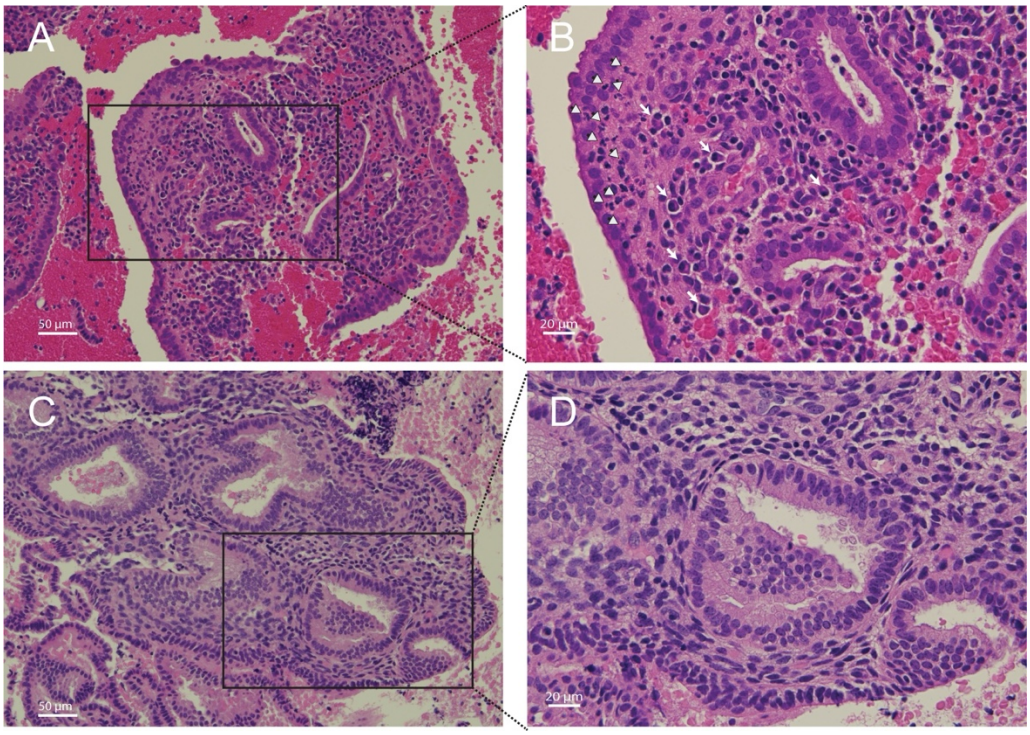

Figure 3. **Histopathology of *Chlamydia trachomatis* endometritis.** (A, 20X; B, 40X) Histological hematoxylin and eosin-stained endometrial tissue sections from a biopsy taken from a woman positive for *C. trachomatis* in their endometrium. White arrows indicate plasma cells; white arrowheads indicate neutrophils. (C, 20X; D, 40X) Endometrial biopsy section from a woman who was negative for endometrial infection but tested positive for *C. trachomatis* infection at their cervix.

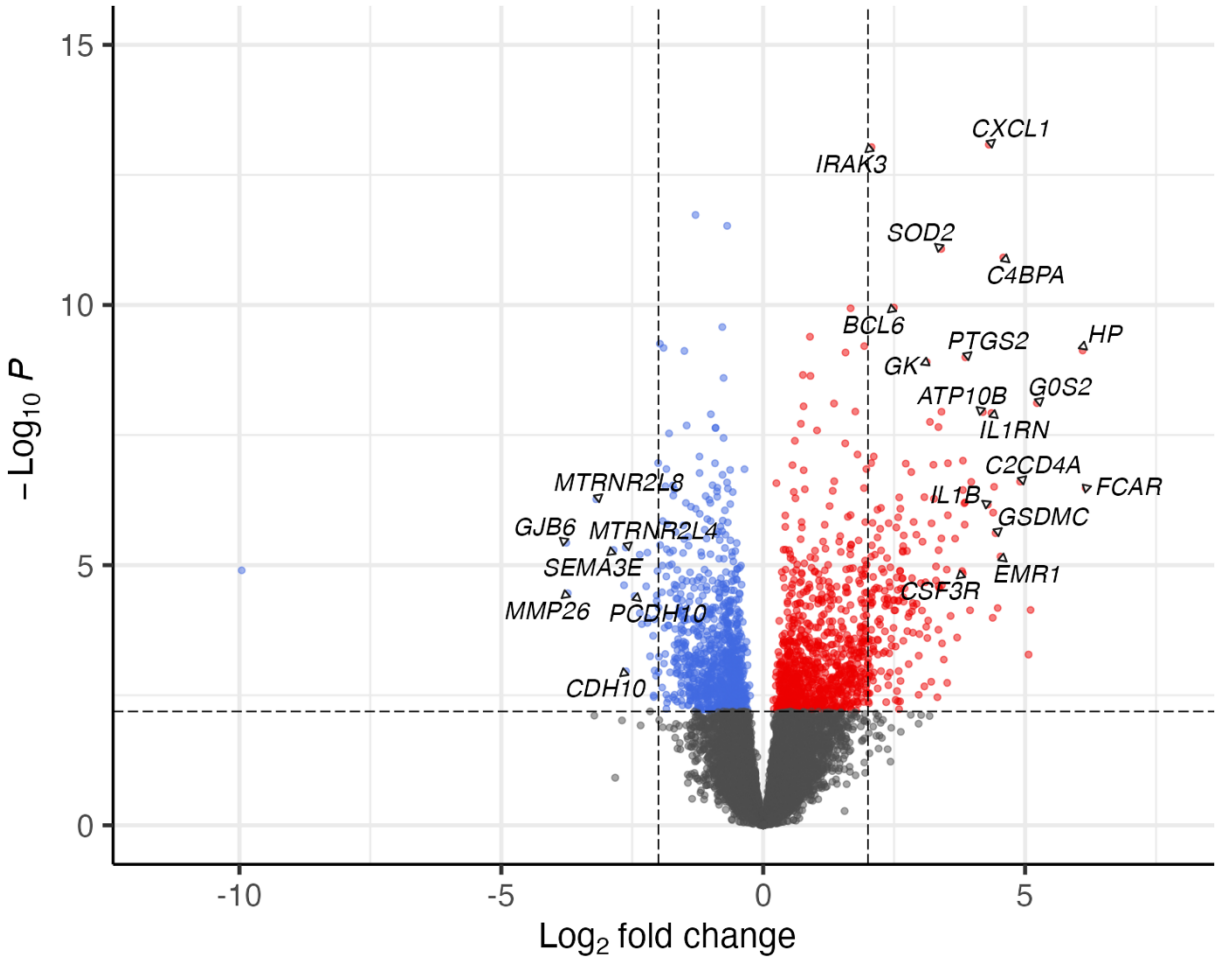

1002

1003 **Figure 4. The significance and fold change of DE mRNAs (FDR<0.05) in Endo+ versus**

1004 **Endo-/Uninfected biopsies depicted by volcano plot.** Each dot represents one mRNA gene,

1005 with red indicating upregulation and blue indicating downregulation in the Endo+ group

1006 compared to the Endo-/Uninfected group. Horizontal dashed line indicates FDR=0.05 (-

1007 $\log_{10}$P=2.2). Left vertical dashed line indicates log2 fold change=-2 (fold change= 0.25) and

1008 right vertical dashed line indicates log2 fold change=2 (fold change=4).

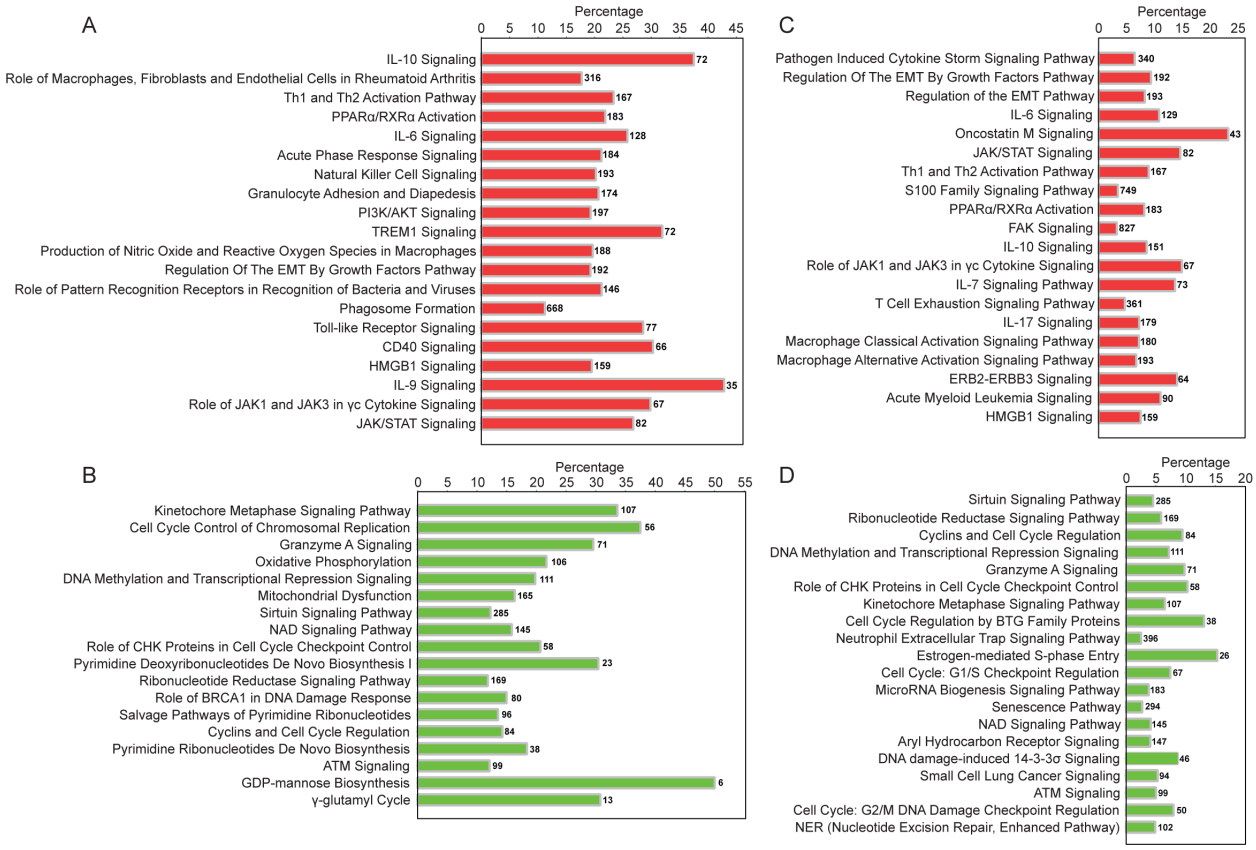

Figure 5. Ingenuity canonical pathways enriched by DE mRNAs and miRNAs in Endo+ compared to Endo-/Uninfected biopsies. (A) Top 20 signaling pathways enriched by significantly upregulated mRNAs in Endo+ biopsies. (B) All 18 pathways enriched by significantly downregulated mRNAs in Endo+ biopsies. (C) Top 20 signaling pathways enriched by downregulated miRNA-upregulated mRNA pairs in Endo+ biopsies. (D) Top 20 signaling pathways enriched by significantly upregulated miRNA-downregulated mRNA pairs in Endo+ biopsies. The percentage is the number of the DE genes present in each pathway, divided by the total number of genes in that pathway according to the IPA database, as listed on the right-hand side of each figure panel.

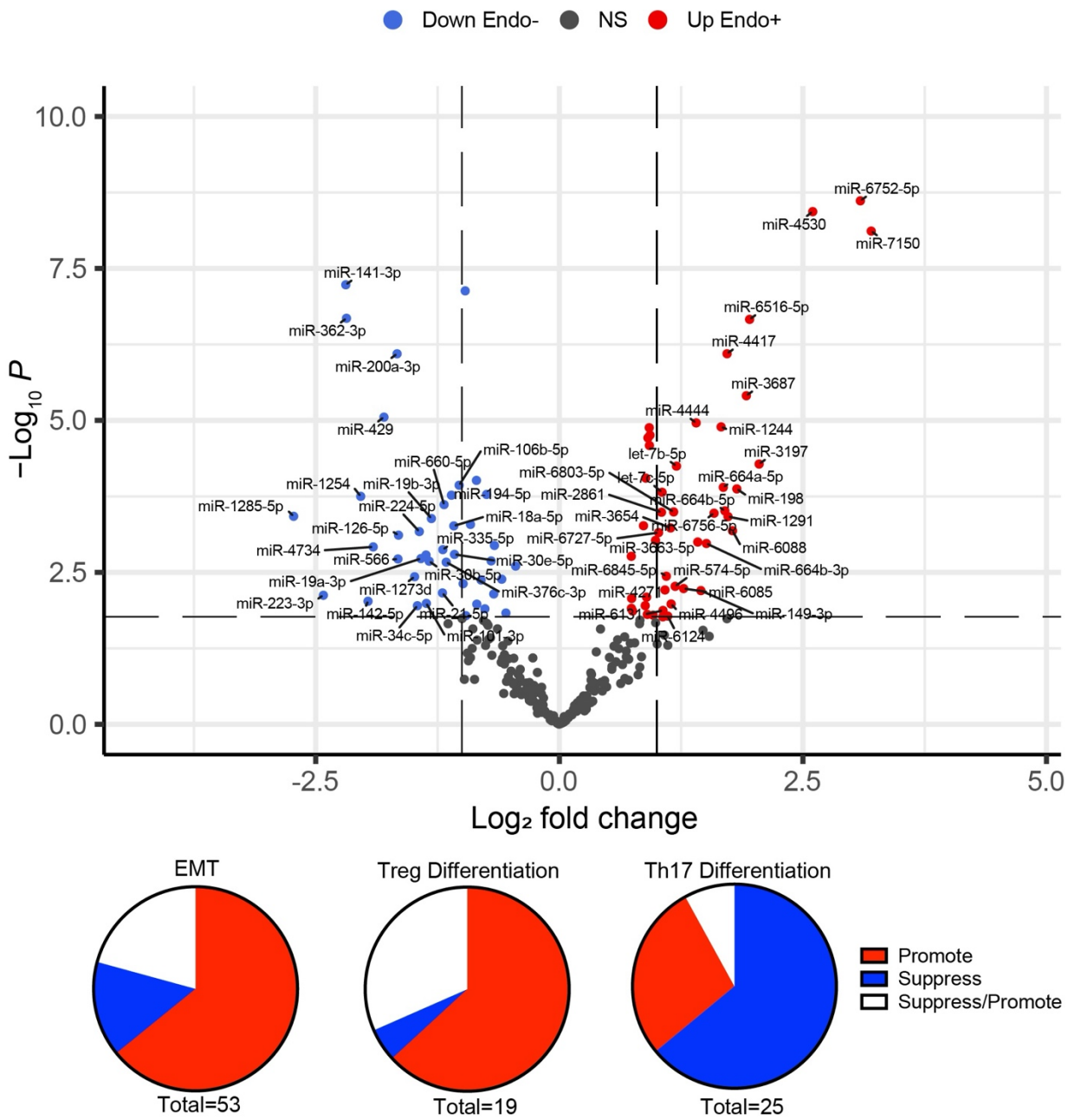

Figure 6. The significance and fold change of DE miRNAs (FDR<0.05) in Endo+ versus Endo-/Uninfected biopsies depicted by (A) volcano plot. Each dot represents one miRNA gene with colors indicating directions of dysregulated expression in the Endo+ group compared to the Endo-/Uninfected group. Horizontal dashed line indicates FDR=0.05 ($-\log_{10}P=2.2$). Left vertical dashed line indicates log2 fold change=-1 (fold changes= 0.5) and right vertical dashed line indicates log2 fold change=1 (fold change=2). All significant DE miRNAs (FDR<0.05) with

1026 fold changes>2 or <0.5 are highlighted. **DE miRNAs linked to (B) EMT, (C) Tregs, and (D)**

1027 **Th17 differentiation are depicted by pie charts.** Red, blue and white colors indicate overall

1028 enhancing, suppressing, and enhancing/suppressing effects of miRNAs, respectively, in Endo+

1029 women compared to Endo-/Uninfected women.

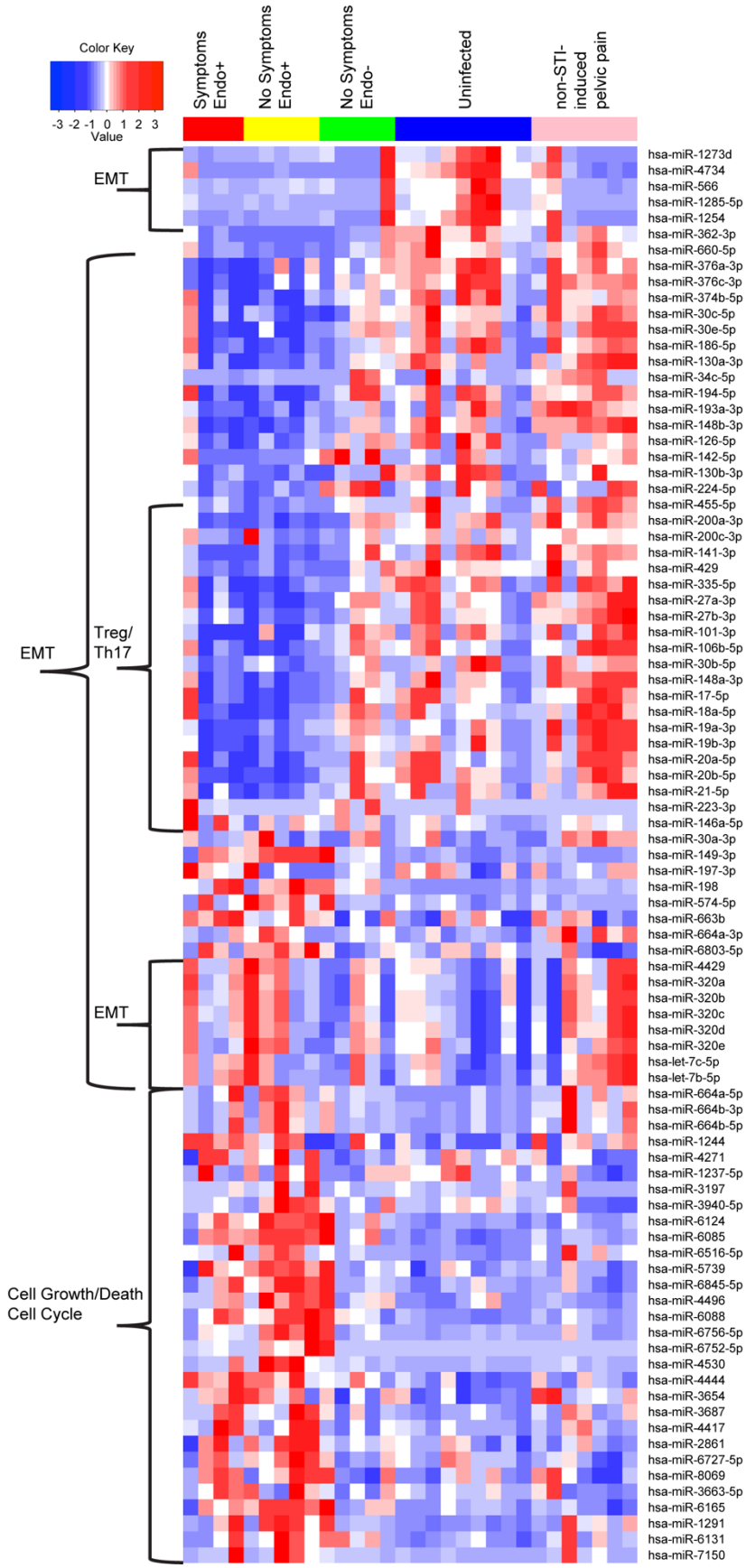
Color Key
-3 -2 -1 0 1 2 3
Value
Symptoms Endo+
No Symptoms Endo+
No Symptoms Endo-
Uninfected
non-STI-induced pelvic pain
EMT
EMT
Treg/ Th17
EMT
Cell Growth/Death
Cell Cycle
hsa-miR-1273d
hsa-miR-4734
hsa-miR-566
hsa-miR-1285-5p
hsa-miR-1254
hsa-miR-362-3p
hsa-miR-660-5p
hsa-miR-376a-3p
hsa-miR-376c-3p
hsa-miR-374b-5p
hsa-miR-30c-5p
hsa-miR-30e-5p
hsa-miR-186-5p
hsa-miR-130a-3p
hsa-miR-34c-5p
hsa-miR-194-5p
hsa-miR-193a-3p
hsa-miR-148b-3p
hsa-miR-126-5p
hsa-miR-142-5p
hsa-miR-130b-3p
hsa-miR-224-5p
hsa-miR-455-5p
hsa-miR-200a-3p
hsa-miR-200c-3p
hsa-miR-141-3p
hsa-miR-429
hsa-miR-335-5p
hsa-miR-27a-3p
hsa-miR-27b-3p
hsa-miR-101-3p
hsa-miR-106b-5p
hsa-miR-30b-5p
hsa-miR-148a-3p
hsa-miR-17-5p
hsa-miR-18a-5p
hsa-miR-19a-3p
hsa-miR-19b-3p
hsa-miR-20a-5p
hsa-miR-20b-5p
hsa-miR-21-5p
hsa-miR-223-3p
hsa-miR-146a-5p
hsa-miR-30a-3p
hsa-miR-149-3p
hsa-miR-197-3p
hsa-miR-198
hsa-miR-574-5p
hsa-miR-663b
hsa-miR-664a-3p
hsa-miR-6803-5p
hsa-miR-4429
hsa-miR-320a
hsa-miR-320b
hsa-miR-320c
hsa-miR-320d
hsa-miR-320e
hsa-let-7c-5p
hsa-let-7b-5p
hsa-miR-664a-5p
hsa-miR-664b-3p
hsa-miR-664b-5p
hsa-miR-1244
hsa-miR-4271
hsa-miR-1237-5p
hsa-miR-3197
hsa-miR-3940-5p
hsa-miR-6124
hsa-miR-6085
hsa-miR-6516-5p
hsa-miR-5739
hsa-miR-6845-5p
hsa-miR-4496
hsa-miR-6088
hsa-miR-6756-5p
hsa-miR-6752-5p
hsa-miR-4530
hsa-miR-4444
hsa-miR-3654
hsa-miR-3687
hsa-miR-4417
hsa-miR-2861
hsa-miR-6727-5p
hsa-miR-8069
hsa-miR-3663-5p
hsa-miR-6165
hsa-miR-1291
hsa-miR-6131
hsa-miR-7150

1030

1031 **Figure 7. A within-sample group hierarchical clustering heatmap of DE miRNAs revealed**
1032 **distinct expression patterns across groups.** Heatmap columns indicate individual patients with
1033 red: Endo+ with pelvic pain; yellow: Endo+ without symptoms; green: Endo- without symptoms;
1034 blue: uninfected without symptoms; pink: pelvic pain without sexually transmitted infection
1035 (STI). Heatmap rows indicate genes. Blue: low expression miRNAs, white: intermediately
1036 expressed miRNAs, and red: highly expressed miRNAs.
1037
1038
1039
1040
1041
1042
1043
1044
1045
1046 Table 1. DE miRNAs in Endo+ compared to Endo- associated with EMT.

DE miRNAs	Fold Change	P value	FDR	Expression changes in Endo+ compared to Endo-	Function of miRNAs	Overall effects	Citations
miR-566	0.32	0.002	0.009	Decrease (-)	↓EMT	**Promote EMT**	(41)
miR-200a-3p	0.32	<0.001	<0.001	Decrease (-)	↓EMT		(42)
miR-200c-3p	0.59	0.013	0.039	Decrease (-)	↓EMT		(42)
miR-141-3p	0.22	<0.001	<0.001	Decrease (-)	↓EMT		(43)
miR-429	0.29	<0.001	<0.001	Decrease (-)	↓EMT		

miR-376a-3p	0.51	0.016	0.048	Decrease (-)	↓EMT		(44)
miR-376c-3p	0.45	0.002	0.009	Decrease (-)	↓EMT		(45)
miR-374b-5p	0.39	0.002	0.008	Decrease (-)	↓EMT		(46)
miR-30b-5p	0.4	0.002	0.009	Decrease (-)	↓EMT		(47)
miR-30c-5p	0.68	0.015	0.045	Decrease (-)	↓EMT		(47)
miR-30e-5p	0.47	0.002	0.008	Decrease (-)	↓EMT		(47)
miR-186-5p	0.62	0.002	0.009	Decrease (-)	↓EMT		(48)
miR-130a-3p	0.63	0.001	0.006	Decrease (-)	↓EMT		(49)
miR-335-5p	0.44	0.001	0.007	Decrease (-)	↓EMT		(50)
miR-17-5p	0.6	<0.001	0.002	Decrease (-)	↓EMT		(51)
miR-18a-5p	0.47	0.001	0.004	Decrease (-)	↓EMT		(51)
miR-19a-3p	0.37	0.002	0.009	Decrease (-)	↓EMT		(51)
miR-19b-3p	0.4	<0.001	0.003	Decrease (-)	↓EMT		(51)
miR-20a-5p	0.5	0.005	0.019	Decrease (-)	↓EMT		(51)
miR-20b-5p	0.51	<0.001	<0.001	Decrease (-)	↓EMT		(52, 53)
miR-34c-5p	0.36	0.011	0.036	Decrease (-)	↓EMT		(54)
miR-101-3p	0.39	0.01	0.035	Decrease (-)	↓EMT		(55)
miR-194-5p	0.46	<0.001	0.002	Decrease (-)	↓EMT		(56)
miR-193a-3p	0.57	0.004	0.017	Decrease (-)	↓EMT		(57)
miR-148a-3p	0.53	0.001	0.004	Decrease (-)	↓EMT		(58, 59)
mir-148b-3p	0.73	0.002	0.011	Decrease (-)	↓EMT		(60)
miR-126-5p	0.32	<0.001	0.004	Decrease (-)	↓EMT		(61, 62)
miR-142-5p	0.26	0.009	0.032	Decrease (-)	↓EMT		(63)
miR-1285-5p	0.15	<0.001	0.003	Decrease (-)	↓EMT		(64)
mir-1254	0.24	<0.001	0.002	Decrease (-)	↓EMT		(65)
miR-6803-5p	2.26	<0.001	0.003	Increase (+)	↑EMT		(66)
miR-664a-3p	1.82	0.001	0.004	Increase (+)	↑EMT		(67)

miR-663b	1.98	0.001	0.005	Increase (+)	↑EMT		(68)
miR-197-3p	1.67	0.012	0.039	Increase (+)	↑EMT		(69)
miR-106b-5p	0.49	<0.001	0.001	Decrease (-)	↑EMT	Suppress EMT	(70-72)
miR-198	3.54	<0.001	0.001	Increase (+)	↓EMT		(73)
mir-30a-3p	1.67	0.008	0.027	Increase (+)	↓EMT		(74)
miR-320a	1.9	<0.001	<0.001	Increase (+)	↓EMT		(75)
miR-320c	1.88	<0.001	<0.001	Increase (+)	↓EMT		(76)
miR-320d	1.85	<0.001	0.001	Increase (+)	↓EMT		(77)
let-7c-5p	2.08	<0.001	0.002	Increase (+)	↓EMT		(78)
miR-4429	1.9	<0.001	<0.001	Increase (+)	↓EMT		(79, 80)
miR-130b-3p	0.63	0.007	0.026	Decrease (-)	↓↑EMT	Suppress/Promote EMT	(81-83)
miR-21-5p	0.6	0.024	0.05	Decrease (-)	↓↑EMT		(84, 85)
miR-27a-3p	0.55	<0.001	0.001	Decrease (-)	↓↑EMT		(86, 87)
miR-27b-3p	0.66	0.004	0.017	Decrease (-)	↓↑EMT		(88, 89)
miR-224-5p	0.37	0.001	0.004	Decrease (-)	↓↑EMT		(90, 91)
miR-455-5p	0.56	0.011	0.035	Decrease (-)	↓↑EMT		(92, 93)
miR-223-3p	0.19	0.008	0.027	Decrease (-)	↓↑EMT		(94)
miR-149-3p	2.74	0.006	0.024	Increase (+)	↓↑EMT		(95, 96)
miR-574-5p	2.28	0.005	0.021	Increase (+)	↓↑EMT		(97, 98)
miR-146a-5p	2.09	0.017	0.048	Increase (+)	↓↑EMT		(99, 100)
miR-320b	1.91	<0.001	<0.001	Increase (+)	↓↑EMT		(75, 101)

Table 3. DE miRNAs in Endo+ compared to Endo-, associated with Th17 cell differentiation.

DE miRNAs	**Fold change**	**P value**	**FDR**	**Expression changes in Endo+ compared to Endo-**	**Function of miRNAs**	**Overall effects**	**Citations**
miR-200a-3p	0.32	8.02E-07	2.25E-05	Reduced (-)	↑ Th17		(105, 106)

miR-141-3p	0.22	5.87E-08	3.71E-06	Reduced (-)	↑ Th17	Suppress Th17 differentiation	(108)
miR-200c-3p	0.59	1.26E-02	3.93E-02	Reduced (-)	↑ Th17		(105)
miR-429	0.29	8.84E-06	2.03E-04	Reduced (-)	↑ Th17		
miR-374b-5p	0.39	1.64E-03	7.98E-03	Reduced (-)	↑ Th17		(123)
miR-106b-5p	0.49	1.17E-04	1.34E-03	Reduced (-)	↑ Th17		(113)
miR-130b-3p	0.63	7.17E-03	2.59E-02	Reduced (-)	↑ Th17		(124)
miR-17	0.60	1.65E-04	1.59E-03	Reduced (-)	↑ Th17		(125)
miR-18a	0.47	5.44E-04	3.53E-03	Reduced (-)	↑ Th17		(125)
miR-19a	0.37	1.88E-03	8.76E-03	Reduced (-)	↑ Th17		(125)
miR-19b	0.4	4.12E-04	2.89E-03	Reduced (-)	↑ Th17		(125)
miR-20a	0.50	4.86E-03	1.92E-02	Reduced (-)	↑ Th17		(125)
mir-30c-5p	0.68	1.48E-02	4.45E-02	Reduced (-)	↑ Th17		(126)
mir-223-3p	0.19	7.53E-03	2.68E-02	Reduced (-)	↑ Th17		(114, 127)
Let-7b	2.3	5.66E-05	7.54E-04	Increased (+)	↓ Th17		(128)
Let-7c	2.1	1.52E-04	1.54E-03	Increased (+)	↓ Th17		(128)
miR-30a-3p	1.7	8.51E-03	2.95E-02	Reduced (-)	↓ Th17	Promote Th17 differentiation	(129)
miR-20a	0.50	4.86E-03	1.92E-02	Reduced (-)	↓ Th17		(125)
miR-20b	0.51	7.39E-08	3.74E-06	Reduced (-)	↓ Th17		(130)
miR-21-5p	0.44	6.90E-03	2.53E-02	Reduced (-)	↓ Th17		(122, 126)
miR-148a	0.53	5.15E-04	3.52E-03	Reduced (-)	↓ Th17		(131) (125)
miR-148b	0.73	2.50E-03	1.07E-02	Reduced (-)	↓ Th17		(132)
miR-149-3p	2.7	6.32E-03	2.35E-02	Increased (+)	↑ Th17		(133)
miR-27 a	0.55	9.72E-05	1.17E-03	Reduced (-)	↓↑ Th17	Suppress/promote Th17 differentiation	(134, 135)
miR-27 b	0.66	4.10E-03	1.67E-02	Reduced (-)	↓↑ Th17		(134, 135)

1049

Table 4. Comparison of pathways enriched by significantly differentially expressed (DE) mRNAs in Endo+ versus Endo- women, as determined from either endometrial biopsy or blood samples#.

IPA Pathway	Endometrium	Blood

	Regulation direction in Endo+	Adjusted P*	Regulation direction in Blood	Adjusted P**
Up-regulated in Endometrium and Blood				
IL-10 Signaling	↑	3.83E-15	↑	1.29E-06
IL-6 Signaling	↑	3.83E-13	↑	1.32E-05
Granulocyte Adhesion and Diapedesis	↑	3.04E-11	↑	6.92E-03
TREM1 Signaling	↑	6.07E-11	↑	7.78E-09
Production of Nitric Oxide and Reactive Oxygen Species in Macrophages	↑	6.07E-11	↑	6.15E-04
PI3K/AKT Signaling	↑	6.07E-11	↑	1.48E-03
Phagosome Formation	↑	1.92E-09	↑	1.66E-04
Toll-like Receptor Signaling	↑	2.42E-09	↑	3.47E-05
IL-8 Signaling	↑	9.84E-08	↑	5.13E-07
IL-3 Signaling	↑	1.71E-06	↑	3.47E-02
IL-17 Signaling	↑	1.30E-05	↑	4.16E-02
Leukocyte Extravasation Signaling	↑	4.20E-05	↑	1.86E-04
IL-1 Signaling	↑	5.29E-03	↑	1.38E-02
Dendritic Cell Maturation	↑	1.63E-02	↑	2.57E-05
Integrin Signaling	↑	1.81E-02	↑	9.34E-04
T Helper Cell Differentiation	↑	2.05E-02	↑	1.02E-03
Interferon Signaling	↑	3.88E-02	↑	1.95E-12
Up-regulated Only in Endometrium				
Th1 and Th2 Activation Pathway	↑	3.04E-14		##NS
Natural Killer Cell Signaling	↑	6.07E-12		NS
Regulation Of The Epithelial Mesenchymal Transition	↑	1.21E-10		NS
IL-23 Signaling Pathway	↑	7.47E-08		NS
IL-7 Signaling Pathway	↑	4.10E-07		NS
STAT3 Pathway	↑	4.50E-07		NS
TGF-β Signaling	↑	1.67E-06		NS
IL-13 Signaling Pathway	↑	3.83E-03		NS
T Cell Exhaustion Signaling Pathway	↑	2.47E-02		NS
Th17 Activation Pathway	↑	3.74E-02		NS
Up-regulated in Endometrium and Down regulated in Blood				
T Cell Receptor Signaling	↑	5.29E-03	↓	8.52E-03
ICOS-ICOSL Signaling in T Helper Cells	↑	2.36E-02	↓	7.78E-04
mTOR Signaling	↑	NS	↓	4.90E-12
Regulation of eIF4 and p70S6K Signaling	↑	NS	↓	3.89E-11

Data from reference (32).

* Bonferroni adjusted P values in endometrium: P*482 for endometrium (482 total pathways).

**Bonferroni adjusted P values in blood: P*389 for blood (389 total pathways).

##NS: Not Significant.

1054 Light gray indicates pathways that were enriched by significantly upregulated genes only in endometrial
1055 biopsy specimens.
1056 Dark gray indicates pathways that were enriched by significantly down-regulated genes only in blood
1057 specimens.
1058